

Assessment of Candidate Molten Salt Coolants for the Advanced High-Temperature Reactor (AHTR)

March 2006

Prepared by

D. F. Williams
L. M. Toth
K. T. Clarno

DOCUMENT AVAILABILITY

Reports produced after January 1, 1996, are generally available free via the U.S. Department of Energy (DOE) Information Bridge:

Web site: <http://www.osti.gov/bridge>

Reports produced before January 1, 1996, may be purchased by members of the public from the following source:

National Technical Information Service
5285 Port Royal Road
Springfield, VA 22161
Telephone: 703-605-6000 (1-800-553-6847)
TDD: 703-487-4639
Fax: 703-605-6900
E-mail: info@ntis.fedworld.gov
Web site: <http://www.ntis.gov/support/ordernowabout.htm>

Reports are available to DOE employees, DOE contractors, Energy Technology Data Exchange (ETDE) representatives, and International Nuclear Information System (INIS) representatives from the following source:

Office of Scientific and Technical Information
P.O. Box 62
Oak Ridge, TN 37831
Telephone: 865-576-8401
Fax: 865-576-5728
E-mail: reports@osti.gov
Web site: <http://www.osti.gov/contact.html>

This report was prepared as an account of work sponsored by an agency of the United States Government. Neither the United States government nor any agency thereof, nor any of their employees, makes any warranty, express or implied, or assumes any legal liability or responsibility for the accuracy, completeness, or usefulness of any information, apparatus, product, or process disclosed, or represents that its use would not infringe privately owned rights. Reference herein to any specific commercial product, process, or service by trade name, trademark, manufacturer, or otherwise, does not necessarily constitute or imply its endorsement, recommendation, or favoring by the United States Government or any agency thereof. The views and opinions of authors expressed herein do not necessarily state or reflect those of the United States Government or any agency thereof.

Nuclear Science and Technology Division

**ASSESSMENT OF CANDIDATE MOLTEN SALT COOLANTS FOR THE
ADVANCED HIGH-TEMPERATURE REACTOR (AHTR)**

D. F. Williams
L. M. Toth
K. T. Clarno

Date Published: March 2006

Prepared by
OAK RIDGE NATIONAL LABORATORY
P.O. Box 2008
Oak Ridge, Tennessee 37831-6283
managed by
UT-Battelle, LLC
for the
U.S. DEPARTMENT OF ENERGY
under contract DE-AC05-00OR22725

CONTENTS

LIST OF FIGURES	v
LIST OF TABLES	vii
ACRONYMS AND ABBREVIATIONS.....	ix
EXECUTIVE SUMMARY	xi
1. INTRODUCTION	1
2. REVIEW OF PROPERTIES	3
2.1 Thermochemical Properties	3
2.1.1 Melting Point.....	3
2.1.2 Vapor Pressure and Vapor Species	14
2.1.3 Density	17
2.1.4 Heat Capacity	20
2.2 Fluid Transport Properties	21
2.2.1 Viscosity.....	21
2.2.2 Thermal Conductivity	26
3. HEAT-TRANSFER COMPARISONS	29
4. NUCLEAR PROPERTIES.....	33
4.1 Parasitic Neutron Capture and Moderation	33
4.2 Reactivity Coefficients	35
4.3 Short-Term Activation.....	39
4.4 Long-Term Activation	41
5. COST OF THE SALT	43
6. CHEMICAL CONSIDERATIONS.....	45
6.1 Background, context, and Purpose	45
6.1.1 Aircraft Nuclear Propulsion (ANP) Project	46
6.1.2 Molten Salt Reactor Experiment	47
6.1.3 Molten Salt Breeder Reactor	48
6.2 Materials for High-Temperature Fluids.....	48
6.3 Chemistry of Molten Fluoride Salt Coolants.....	50
6.3.1 Salt Purification.....	50
6.3.2 Phase-Diagram Behavior	51
6.3.3 Acid-Base Chemistry	51
6.3.4 Corrosion Chemistry	54
6.4 Coolant Salt Selection Factors Related to Corrosion.....	55
6.4.1 Oxidation State of Corrosion Products.....	55
6.4.2 Temperature Dependence of Dissolved Chromium Concentration	56
6.4.3 Polythermal Corrosion Test Loops with Coolant Salts	56
6.4.4 Redox Control Factors	57

7. CONCLUSIONS AND RECOMMENDATIONS	58
7.1 Conclusions	58
7.2 Recommendations	59
7.3 Candidate Salts	60
7.4 Future Work.....	61
8. REFERENCES	62
APPENDIX	67

LIST OF FIGURES

1.	Binary phase diagrams of BeF ₂ systems.....	6
2.	Binary phase diagrams of alkali fluoride systems.	7
3.	Binary phase diagrams of ZrF ₄ salt systems.....	8
4.	Ternary phase diagram for LiF-NaF-ZrF ₄	11
5.	Ternary phase diagram for RbF-NaF-ZrF ₄	12
6.	Liquidus temperatures for RbF-NaF-ZrF ₄ system with Na:Rb = 1.44	13
7.	ZrF ₄ “snow trap” designs developed for the Aircraft Reactor Test.. ..	15
8.	Vapor pressure trends in alkali fluoride-BeF ₂ systems at 900°C.....	16
9.	Vapor pressure trends in alkali fluoride-ZrF ₄ systems at 900°C.	17
10.	Range of viscosities of various salt systems.....	22
11.	Effect of BeF ₂ composition on the viscosity of LiF-BeF ₂ mixtures at 600°C.....	23
12.	Effect of alkali composition on the viscosity in BeF ₂ salts.	23
13.	Composition effects on viscosity in ZrF ₄ mixtures.....	25
14.	Comparison of values measured for the viscosity of LiF-NaF-KF eutectic	25
15.	Comparison of values measured for the viscosity of NaF-ZrF ₄ , 50-50 mol %.....	26
16.	Activity levels for candidate coolants and comparison coolants	40
17.	Activity levels for components of various salt options.....	40
18.	Effect of redox potential on tellurium cracking of Hastelloy N	50
19.	Activity coefficients of various components versus LiF content, showing acid-base effects on metal ions in solution.....	53

LIST OF TABLES

A.	Summary of the properties of candidate coolants for the AHTR	xiii
B.	Qualitative assessment of properties database and predictive methods.....	xiv
C.	Preliminary ranking of nuclear properties for candidate salt constituents.....	xiv
1.	Grimes' list of elements for molten salt systems.....	2
2.	Useful low freezing salt compositions for AHTR coolants.....	5
3.	Boiling and freezing points of salt compounds and key mixtures.....	14
4.	Salt density equations developed from experimental studies	18
5.	Standard molar volumes for use in estimation of mixture density	19
6.	Salt density by method of additive molar volumes for candidate coolants not previously measured	19
7.	Experimental and estimated values of heat capacity for key salts.....	21
8.	Comparison of measured and predicted thermal conductivities	28
9.	Properties of comparison coolants and candidate coolants at 700°C	29
10.	Turbulent convection and heat exchanger area figures of merit.....	31
11.	Natural convection figures of merit.....	32
12.	Neutronic efficiency for comparison materials and candidate coolants	34
13.	Reactivity coefficients for coolant loss.....	36
14.	Reactivity coefficients for AHTR with 900°C inlet.....	37
15.	Effect of key core design parameters on AHTR reactivity coefficients	38
16.	Nominal activity of coolant constituents after 1 year of decay	42
17.	Nominal activity of coolant constituents after 10 years of decay.....	42
18.	Price estimate of salt coolants in 1971 (U.S. dollars).....	44
19.	Commodity prices for selected materials	44
20.	Predominant oxidation states of dissolved alloy constituents in various molten salts	56
21.	Equilibrium level of dissolved metals for pure elements in contact with various fuel salts	57
A-1	Summary of corrosion testing results for salts without uranium.....	67

ACRONYMS AND ABBREVIATIONS

AHTR	Advanced High-Temperature Reactor
ANP	Aircraft Nuclear Propulsion
ARE	Aircraft Reactor Experiment
ART	Aircraft Reactor Test
CVR	coolant-void ratio
FOM	figure of merit
LLW	low-level waste
LMFBR	Liquid-Metal Fast Breeder Reactor
LS-VHTR	Liquid-Salt-Cooled Very High-Temperature Reactor
MSRE	Molten Salt Reactor Experiment
MSBR	Molten Salt Breeder Reactor
ORNL	Oak Ridge National Laboratory
TRISO	Tristructural Isotropic
VHTR	Very High-Temperature Reactor

EXECUTIVE SUMMARY

The Advanced High-Temperature Reactor (AHTR) is a novel reactor design that utilizes the graphite-matrix high-temperature fuel of helium-cooled reactors, but provides cooling with a high-temperature fluoride salt. For applications at temperatures greater than 900°C the AHTR is also referred to as a Liquid-Salt-Cooled Very High-Temperature Reactor (LS-VHTR). This report provides an assessment of candidate salts proposed as the primary coolant for the AHTR based upon a review of physical properties, nuclear properties, and chemical factors. The physical properties most relevant for coolant service were reviewed. Key chemical factors that influence material compatibility were also analyzed for the purpose of screening salt candidates.

Some simple screening factors related to the nuclear properties of salts were also developed. The moderating ratio and neutron-absorption cross-section were compiled for each salt. The short-lived activation products, long-lived transmutation activity, and reactivity coefficients associated with various salt candidates were estimated using a computational model.

Table A presents a summary of the properties of the candidate coolant salts. Certain factors in this table, such as melting point, vapor pressure, and nuclear properties, can be viewed as stand-alone parameters for screening candidates. Heat-transfer properties are considered as a group in Sect. 3 in order to evaluate the combined effects of various factors. In the course of this review, it became apparent that the state of the properties database was strong in some areas and weak in others. A qualitative map of the state of the database and predictive capabilities is given in Table B. It is apparent that the property of thermal conductivity has the greatest uncertainty and is the most difficult to measure. The database, with respect to heat capacity, can be improved with modern instruments and modest effort.

In general, “lighter” (low- Z) salts tend to exhibit better heat transfer and nuclear performance metrics. Lighter salts also tend to have more favorable (larger) moderating ratios, and thus should have a more favorable coolant-voiding behavior in-core. Heavy (high- Z) salts tend to have lower heat capacities and thermal conductivities and more significant activation and transmutation products. However, all of the salts are relatively good heat-transfer agents. A detailed discussion of each property and the combination of properties that served as a heat-transfer metric is presented in the body of this report.

In addition to neutronic metrics, such as moderating ratio and neutron absorption, the activation properties of the salts were investigated (Table C). Again, lighter salts tend to have more favorable activation properties compared to salts with high atomic-number constituents. A simple model for

estimating the reactivity coefficients associated with a reduction of salt content in the core (voiding or thermal expansion) was also developed, and the primary parameters were investigated. It appears that reasonable design flexibility exists to select a safe combination of fuel-element design and salt coolant for most of the candidate salts.

Materials compatibility is an overriding consideration for high-temperature reactors; therefore the question was posed whether any one of the candidate salts was inherently, or significantly, more corrosive than another. This is a very complex subject, and it was not possible to exclude any fluoride salts based on the corrosion database. The corrosion database clearly indicates superior container alloys, but the effect of salt identity is masked by many factors which are likely more important (impurities, redox condition) in the testing evidence than salt identity. Despite this uncertainty, some reasonable preferences can be recommended, and these are indicated in the conclusions. The reasoning to support these conclusions is established in the body of this report.

Table A. Summary of the properties of candidate coolants for the AHTR

Salt ^a	Formula weight (g/mol)	Melting point (°C)	900°C vapor press (mm Hg)	Heat transfer properties at 700°C				Neutron capture relative to graphite ^b	Moderating ratio ^c
				ρ Density (g/cm ³)	ρ *Cp Volumetric heat capacity (cal/cm ³ -°C)	Viscosity (cP)	Thermal conductivity (W/m-K)		
LiF-BeF ₂	33.0	460	1.2	1.94	1.12	5.6	1.0	8	60
NaF-BeF ₂	44.1	340	1.4	2.01	1.05	7	0.87	28	15
LiF-NaF-BeF ₂	38.9	315	1.7	2.00	0.98	5	0.97	20	22
LiF-ZrF ₄	95.2	509	77	3.09	0.90	> 5.1	0.48	9	29
NaF-ZrF ₄	92.71	500	5	3.14	0.88	5.1	0.49	24	10
KF-ZrF ₄	103.9	390	--	2.80	0.70	< 5.1	0.45	67	3
Rb-ZrF ₄	132.9	410	1.3	3.22	0.64	5.1	0.39	14	13
LiF-NaF-ZrF ₄	84.2	436	~ 5	2.79	0.84	6.9	0.53	20	13
LiF-NaF-KF	41.3	454	~ 0.7	2.02	0.91	2.9	0.92	90	2
LiF-NaF-RbF	67.7	435	~ 0.8	2.69	0.63	2.6	0.62	20	8

^a Salt compositions are given in Table 2; nuclear calculations used 99.995% ⁷Li.

^b Computations based on energy range 0.1 to 10 eV (Sect. 4.1)

^c As defined in textbooks and in Sect. 4.1.

Table B. Qualitative assessment of properties database and predictive methods

Prediction method	Accurate	Approximate	Difficult to predict
Measurement			
accurate	<i>Density</i>		<i>Melting point</i> <i>Vapor pressure</i> <i>Viscosity</i>
database is deficient*		<i>Heat capacity</i>	
poor database difficult to measure			<i>Thermal conductivity</i>

* Better measurement methods exist since the database was populated.

Table C. Preliminary ranking of nuclear properties for candidate salt constituents

	Moderating ratio	Short-lived activation	Long-lived activation
Lithium	Good	Very good	Very good
Beryllium	Very good	Very good	Good
Fluorine	Very good	Very good	Very good
Sodium	Acceptable	Acceptable	Good
Potassium	Poor	Acceptable	Poor
Rubidium	Acceptable	Poor	Good
Zirconium	Good	Poor	Acceptable

1. INTRODUCTION

The Advanced High-Temperature Reactor (AHTR) is a novel reactor design that utilizes the graphite-matrix high-temperature fuel of helium-cooled reactors, but provides cooling with a high-temperature fluoride salt [1,2]. The purpose of this report is to provide a critical review of relevant properties of candidate salts for use in the evaluation and ranking of coolants for the AHTR. Considerable experience exists with molten salts; however, previous nuclear experience with molten salts was for reactor systems that contained fissile and fertile material in the primary fluid (which served as both fuel and primary coolant). The AHTR uses solid fuel and “clean” coolant salt. Also, the AHTR is expected to operate at much higher temperatures than previous applications. Hence, the property and composition requirements may be quite different than those for previous applications, and a new assessment of options is required.

High-temperature operation ($>700^{\circ}\text{C}$) and new compositions have been evaluated based on open literature and internal reports available to the authors, and on use of the best available estimation techniques. Recommended estimation methods are identified when possible, and measurement techniques are briefly discussed when necessary. A number of salt compositions have been examined in detail in previous studies—e.g., eutectic compositions of LiF-BeF_2 , NaF-BeF_2 , LiF-NaF-KF , and NaF-ZrF_4 . These salt systems serve as endpoints for an investigation of more complex systems that can offer more favorable properties.

The screening logic for selecting primary and secondary salt coolants established by Grimes [3,4] many years ago still applies to the selection of the AHTR coolant. Grimes’ basic conclusions remain true today; however, the evaluation criteria are slightly different for a primary coolant application. Grimes first considered all the elements that could possibly be used in a molten salt coolant based on thermal neutron-capture cross-sections (values <1 barn). This list is shown in Table 1. He then applied a number of additional screening criteria to candidate compounds. Grimes required that elements must form compounds that:

1. exhibit chemical stability at $T > 800^{\circ}\text{C}$,
2. are stable under intense radiation,
3. melt at useful temperatures ($<525^{\circ}\text{C}$) and are not volatile,
4. are compatible with high-temperature alloys and graphite, and
5. dissolve useful quantities of fertile and fissile material.

Table 1. Grimes' list of elements for molten salt systems

Element or isotope	Thermal cross-section (barns)	Reason for exclusion of possible compounds
Nitrogen-15	0.000024	Stability and compatibility
Oxygen	0.0002	Stability and compatibility
Deuterium	0.00057	Stability and compatibility
Hydrogen	0.33	
Carbon	0.0033	No thermo-stable liquids
Fluorine	0.009	<i>OK – suitable salts exist</i>
Beryllium	0.010	<i>OK – suitable salts exist</i>
Bismuth	0.032	Not compatible with alloys
Lithium-7	0.033	<i>OK – suitable salts exist</i>
Boron-11	0.05	<i>OK – suitable salts exist</i>
Magnesium	0.063	No low-melting salts exist
Silicon	0.13	Not compatible with alloys
Lead	0.17	Not compatible with alloys
Zirconium	0.18	<i>OK – suitable salts exist</i>
Phosphorus	0.21	Stability and compatibility
Aluminum	0.23	No low-melting nonvolatile salts
Rubidium	0.37	<i>OK – suitable salts exist</i>
Calcium	0.43	No low-melting salts exist
Sulfur	0.49	Stability and compatibility
Sodium	0.53	<i>OK – suitable salts exist</i>
Chlorine-37	0.56	Less attractive than F; requires ⁷ Li
Tin	0.6	Not compatible with alloys
Cerium	0.7	No low-melting salts exist

Only the last item (#5) does not apply to the AHTR primary coolant. The omission of this requirement does not affect the elements that can be considered; rather, it broadens the list of potential candidate mixtures of these elements. The results of this screening process are shown in Table 1.

Three basic salt systems exhibit usefully low melting points and also have the potential for neutronic viability and materials compatibility with alloys: (1) alkali fluoride salts, (2) ZrF₄-containing salts, and (3) BeF₂-containing salts. These three families of salts are the basis for the examination of properties in this report. Other coolants (water, liquid metals, and additional salts) are included as a basis for heat-transfer comparisons in Sect. 3, even though they are not suitable candidates for the AHTR coolant.

2. REVIEW OF PROPERTIES

2.1 THERMOCHEMICAL PROPERTIES

2.1.1 Melting Point

Without question, the melting (or freezing) point is the single most important physical property for a candidate coolant. The requirement for a low freezing temperature depends, to some degree, on the system design, and especially on the power-generation machinery. Because salt coolants possess high heat capacity, the temperature drop in the primary loop is typically small — between 50 and 100°C. For the design and operation of salt-fueled reactors, such as the Aircraft Reactor Experiment (ARE), the Molten Salt Reactor Experiment (MSRE), and the Molten Salt Breeder Reactor (MSBR), a requirement was established that the primary-salt freeze temperature should provide a significant temperature margin ($>100^{\circ}\text{C}$) to freezing throughout the plant. Thus, fuel-containing salts, which also served as the primary coolant for fluid-fueled designs, were required to have freezing points below 525°C to be considered useful [4]. The 525°C limit was also dictated by the need for the primary coolant to exchange heat in a practical manner with the secondary coolant. The previous generation of secondary coolant salts were expected to operate in a steam generator, so a secondary-salt freezing point less than 400°C was required [5].

The situation for the AHTR is different from that of these fluid-fueled systems, but some useful analogies can be drawn. We do not know exactly what the power-generation machinery or heat-transfer loop will require of a secondary coolant, thus we cannot predict exactly what the freezing point requirements will be for the primary coolant. However, we can assume that a high-temperature reactor of the type envisioned by the AHTR will use gas turbines of some type for the highest-temperature portion of the power-generation machinery and will not require freezing points as low as those required by steam systems.

Therefore, while the requirement for a low freezing point is not as fundamental a constraint for the AHTR system as for previous systems, it will still be highly desirable for the purposes of having cheaper materials and simpler systems everywhere in the plant. The requirements for the freezing point for AHTR coolant will probably exist somewhere between the limits established previously for the MSBR fuel salt (525°C) and secondary salt (400°C). Because molten salts are a new technology for the nuclear industry, it is highly desirable to use a system with as low a freezing point as possible in order to simplify the materials, components, and system requirements. Salts that freeze below 400°C should be given priority, all other factors being equal.

An extensive database of phase diagrams exists for salt systems of all types [6,7]; therefore, there is very little need to pursue estimation techniques. Because no single-component salt freezes at a sufficiently low temperature, multicomponent mixtures of salts are required. Nearly all of the binary phase diagrams of interest have been measured, and many of the ternary systems have also been investigated. In general, the primary lowering of the freezing point (as much as 500°C) occurs with the addition of the first salt to a pure component. Additional lowering of the freezing point can be achieved by adding a third component, but these freezing-point depressions are of a lower order (~50°C). Additional components are typically important for reasons other than lowering of the freezing point (e.g., cost, neutronics, or some other physical property).

The families of fluorides that are useful for primary coolant applications have already been identified [8]: (a) alkali-fluorides, (b) ZrF₄-salt mixtures, and (c) BeF₂-salt mixtures. Table 2 lists the primary eutectic compositions in each family in order of freezing point. Simplified phase diagrams [9] of the most important binary systems are included in Figs. 1–3.

In creating the list in Table 2, we excluded certain compositions for reasons that may not be readily apparent. For example, in the phase diagram of BeF₂ systems, there exist very low freezing-temperature compositions in the BeF₂-rich region, and it would be natural to include these in a list of low-freezing candidates. However, experience has demonstrated that these BeF₂-rich systems are not good candidates because they are very viscous due to the associative behavior of BeF₂ in these mixtures. Table 2 also includes some systems normally excluded from consideration as primary coolants. Potassium-containing salts are usually excluded from consideration as a primary coolant because of the relatively large parasitic capture cross-section of potassium. However, potassium-containing salts are commonly used in non-nuclear applications and serve as a useful frame of reference (e.g., FLiNaK). As can be seen in Table 2, in all cases, there are rubidium analogs to the potassium systems that have freezing points close to that of corresponding potassium systems. Rubidium has a parasitic thermal neutron-capture cross-section much lower than potassium; however, it also possesses epithermal resonance absorption bands.

Table 2. Useful salt compositions for AHTR coolants

<i>Alkali fluorides</i>	<i>ZrF₄ salts</i>	<i>BeF₂ salts</i>
	LiF-ZrF₄ (51-49) 509°C	
	NaF-ZrF₄ (59.5-40.5) 500°C	
LiF-KF (50-50) 492°C		
LiF-RbF (44-56) 470°C		
LiF-NaF-KF (“FLiNaK”) (46.5-11.5-42) 454°C	LiF-NaF-ZrF ₄ (42-29-29) 460°C	LiF-BeF₂ (“FLiBe”) (67-33) 460°C
LiF-NaF-RbF (42-6-52) 435°C	LiF-NaF-ZrF ₄ (26-37-37) 436°C NaF-RbF-ZrF ₄ (33-24-43) 420°C	LiF-BeF ₂ -ZrF ₄ (64.5-30.5-5) 428°C
	RbF-ZrF₄ (58-42) 410°C	
	KF-ZrF₄ (58-42) 390°C	
		NaF-BeF₂ (57-43) 340°C LiF-NaF-BeF ₂ (31-31-38) 315°C

Note: Primary binary compositions are shown in bold.

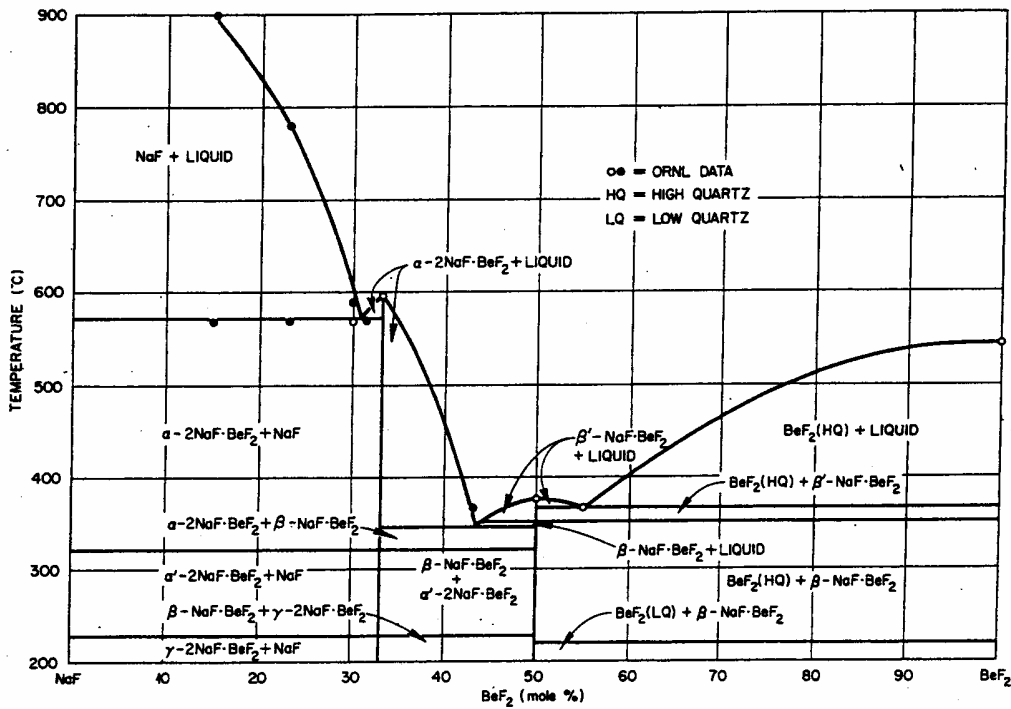
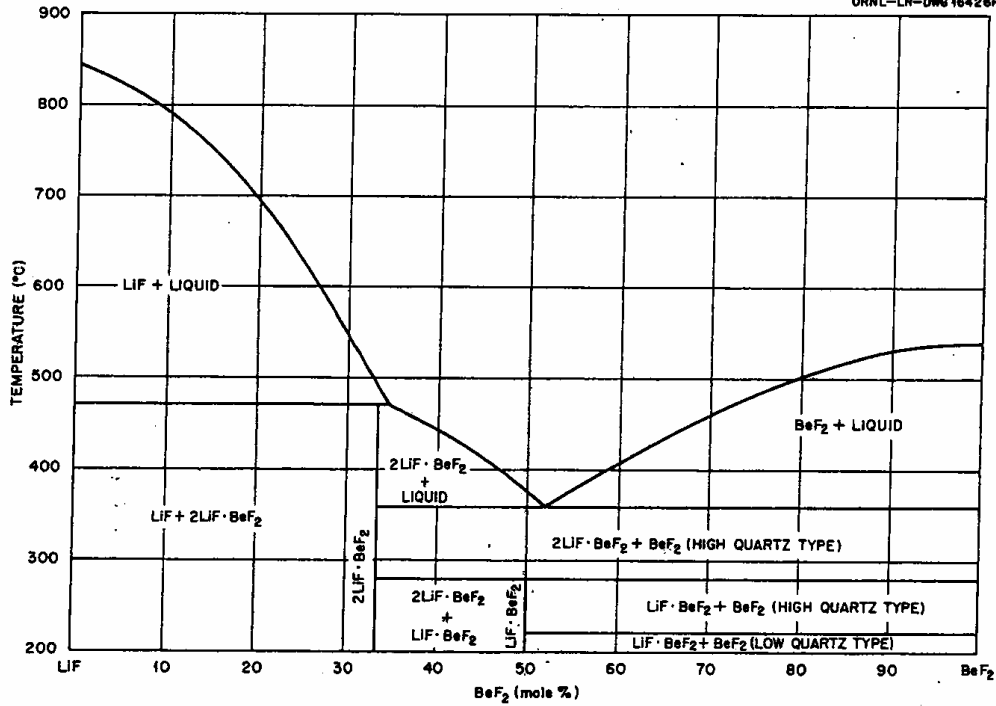


Fig. 1. Binary phase diagrams of BeF_2 systems.

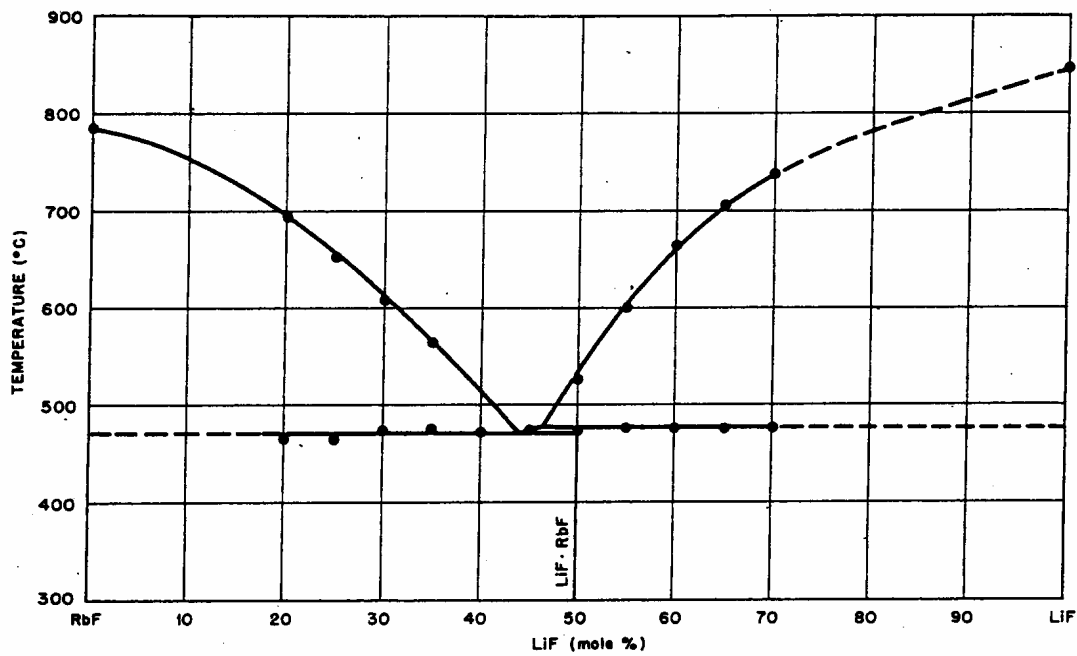
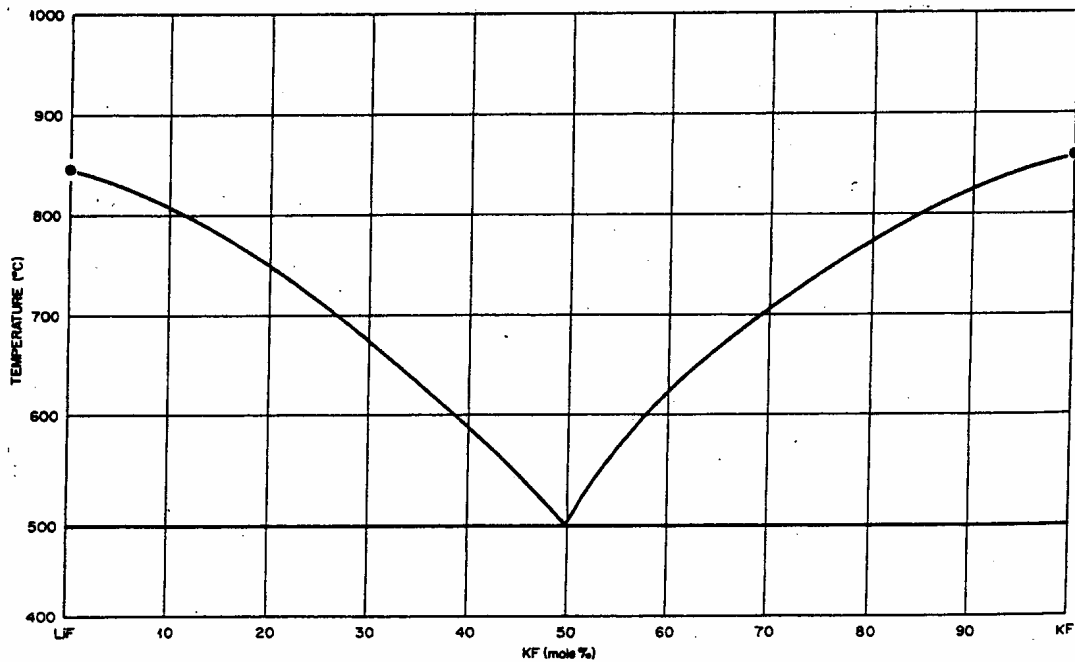


Fig. 2. Binary phase diagrams of alkali fluoride systems.

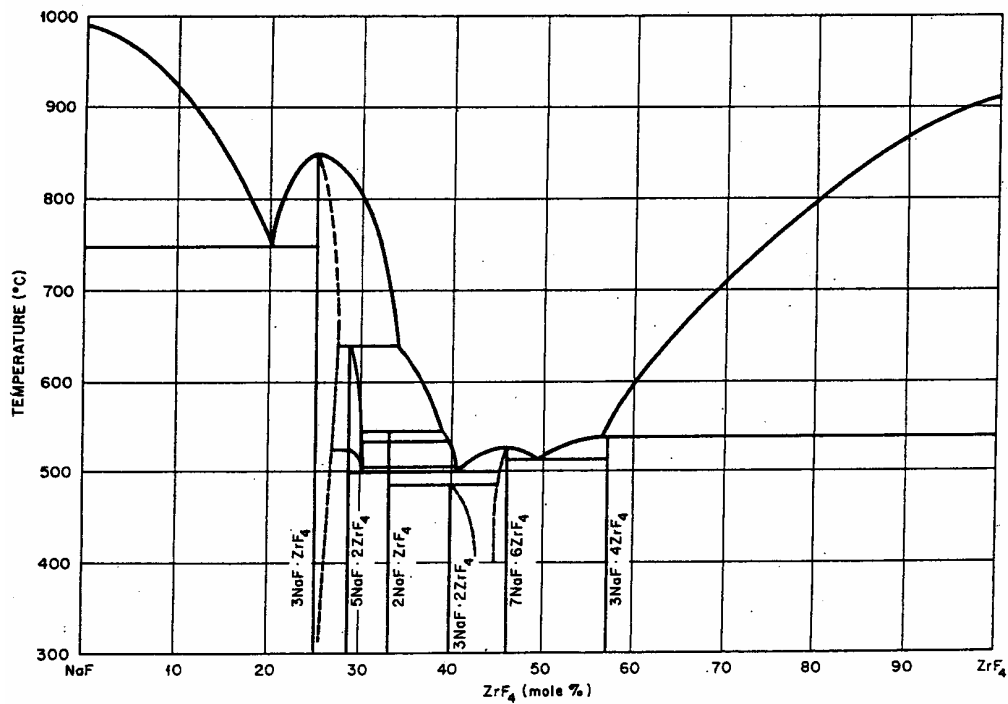
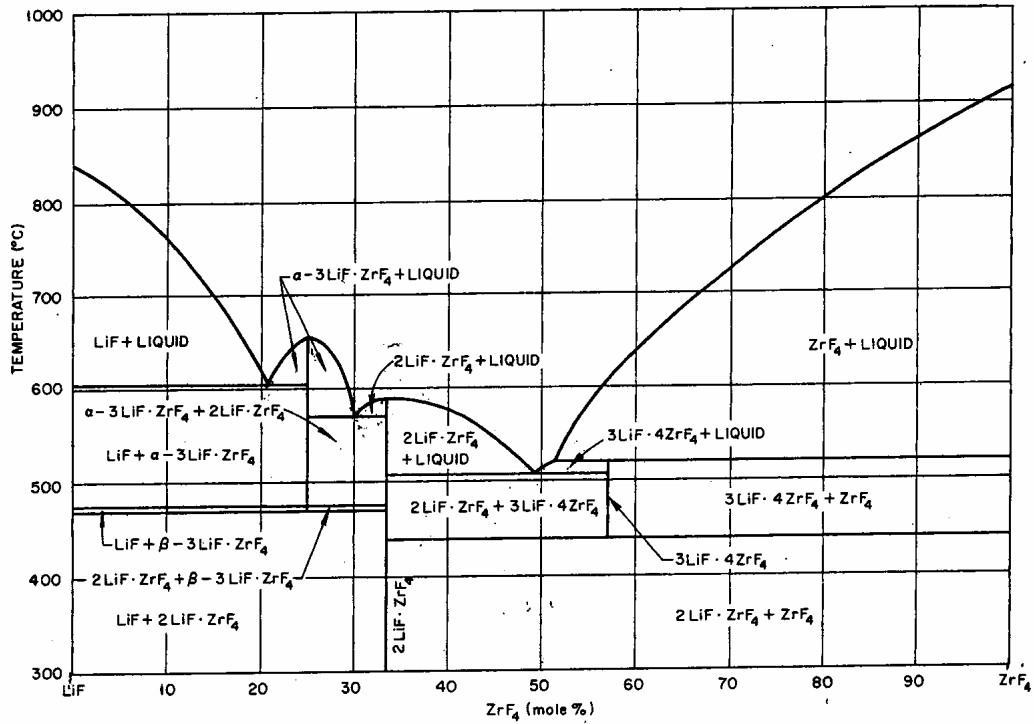


Fig. 3. Binary phase diagrams of ZrF_4 salt systems.

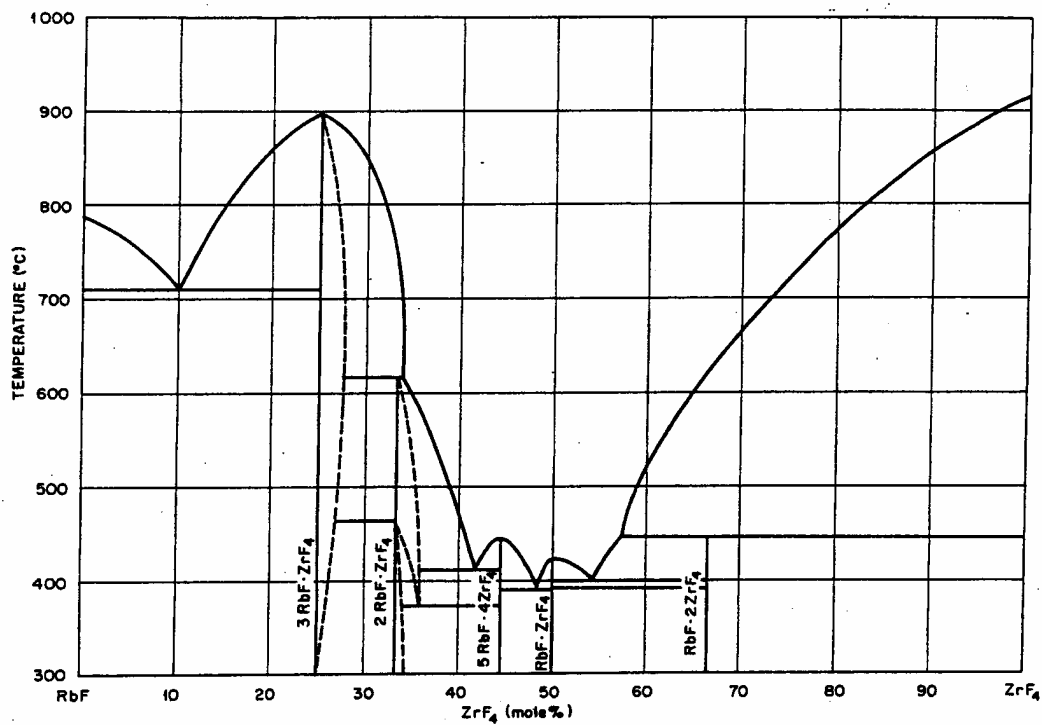
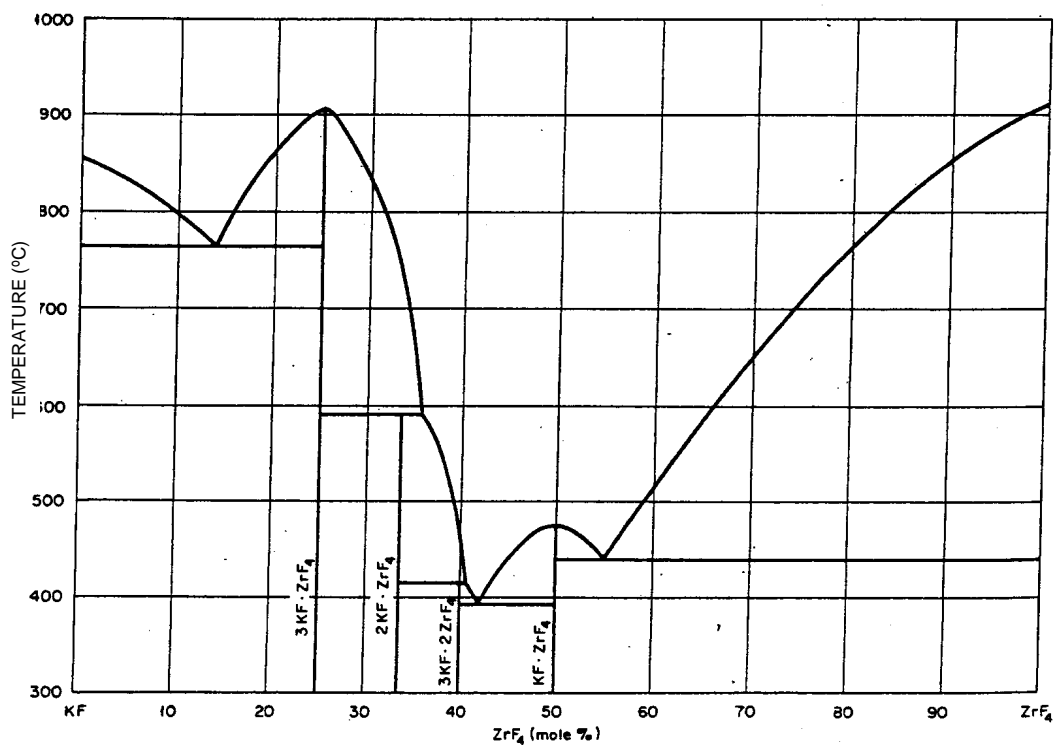


Fig. 3 (cont.). Binary phase diagrams of ZrF₄ salt systems.

A discussion of ternary systems requires that we introduce some of the material on vapor pressure developed in the next section. The desirability of considering ternary salt systems is discussed below for each family of salts.

The alkali fluorides possess simple ternary low-melting eutectic compositions listed in Table 2; therefore, phase diagrams do not need to be examined. These ternary systems possess only modest melting point depressions ($\sim 40^\circ\text{C}$) compared to the binary eutectics. The ternary eutectic compositions are favored in preference to the binary eutectics because they substitute inexpensive NaF for expensive ^7LiF and neutron-absorbing KF. The ternary eutectic in the LiF-NaF-BeF₂ system possesses a 25°C melting-point depression compared to the NaF-BeF₂ eutectic, but this mixture does not seem useful as a coolant because it does not offer a significant advantage over the NaF-BeF₂ eutectic, and yet it requires the addition of an expensive component: ^7LiF .

The ternary systems containing ZrF₄ offer more promising possibilities. The ternary eutectic in the LiF-NaF-ZrF₄ system possesses a large phase field (Fig. 4) with melting points below 500°C , and distinct eutectic compositions at a Na:Zr ratio of 1. These ternary eutectics (42-29-29 and 26-37-37 mol %) are the most promising candidate coolants because (a) they maintain ZrF₄ <40 mol % (necessary for low vapor pressure) and (b) they provide a significant melting point depression ($40\text{--}64^\circ\text{C}$) compared to the NaF-ZrF₄ binary system. The eutectic composition of 30-24-46 is not favored because it offers little melting point advantage and yet still imposes high ZrF₄ vapor pressures and significant ^7Li content.

The NaF-RbF-ZrF₄ ternary system, (shown in Fig. 5) also possesses some attractive compositions with low melting points. The advantage of replacing RbF with NaF is that NaF is relatively inexpensive, it has a lower effective neutron cross-section than RbF, and compositions with lower ZrF₄ content (and thus lower vapor pressure) can be considered. The very lowest melting point regions ($T < 400^\circ\text{C}$) shown in Fig. 5 are not significantly different than the RbF-ZrF₄ eutectic compositions. The eutectic regions in the neighborhood of Na:Rb = 1.44 have a number of interesting properties. Quite a few eutectic mixtures exist with melting points in the neighborhood of $420\text{--}430^\circ\text{C}$. Figure 6 displays the liquidus temperatures along the line Na:Rb = 1.44, and indicates a minimum melting point region in the neighborhood of ZrF₄ = 39–43 mol %. A composition of 33-23.5-43.5 melting at 420°C was selected as a candidate coolant because it is likely to have the best neutronic behavior among these particular compositions.

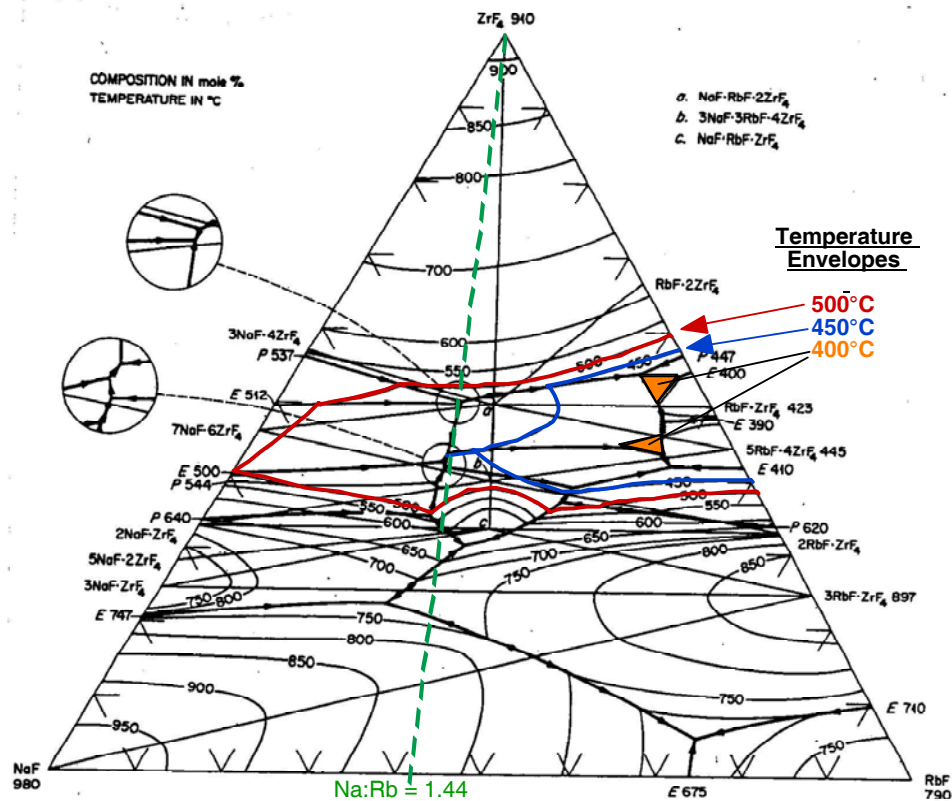


Fig. 5. Ternary phase diagram for RbF-NaF-ZrF₄.

Mol %					Mol %				
NaF	RbF	ZrF ₄	T (°C)	Phase transition type	NaF	RbF	ZrF ₄	T (°C)	Phase transition type
23	72	5	643	Eutectic	23.5	39.5	37	470	Peritectic
50	27	23	720	Eutectic	21	40	39	438	Peritectic
37	32	31	605	Eutectic	8	50	42	400	Eutectic
39	26	35	545	Peritectic	8.5	47	44.5	395	Eutectic
36.3	24.2	39.5	427	Peritectic	6.2	45.8	48	380	Eutectic
34.5	24	41.5	424	Peritectic	5	42	53	398	Eutectic
33	23.5	43.5	420	Eutectic	6.5	39	54.5	423	Peritectic
28.5	21.5	50	443	Eutectic	33.3	33.3	33.3	642	Congruent melt
28	21.5	50.5	446	Eutectic	25	25	50	462	Congruent melt

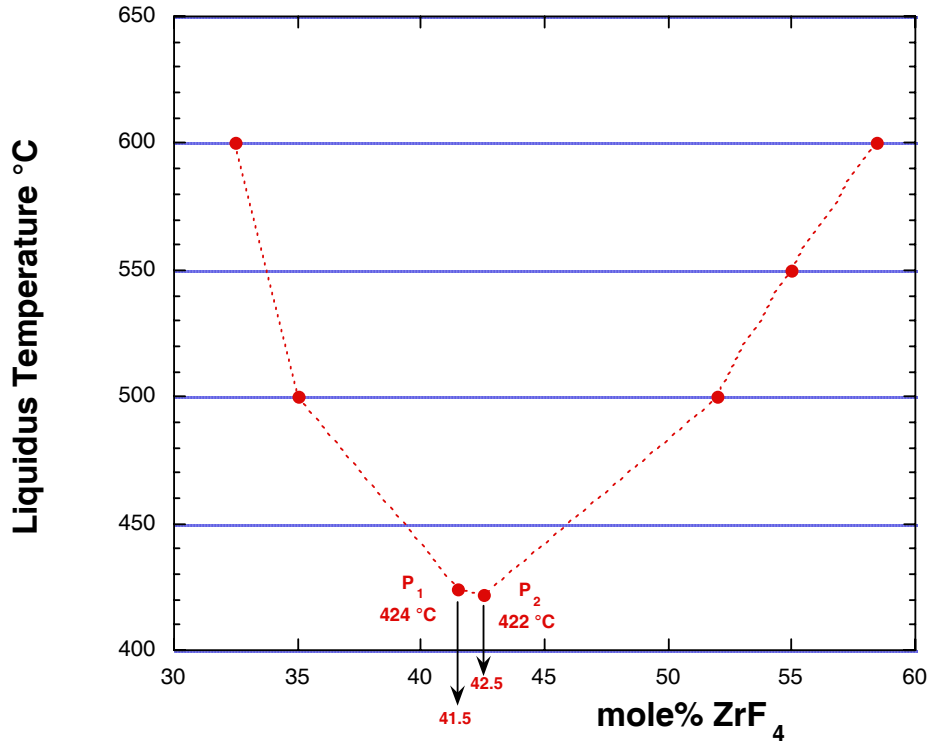


Fig. 6. Liquidus temperatures for RbF-NaF-ZrF₄ system with Na:Rb = 1.44.

It should be noted that all of the systems containing lithium will require highly enriched ⁷Li. In the family of alkali-fluoride salts, all of the mixtures with acceptable freezing points contain lithium. The BeF₂ and ZrF₄ families of salts possess low-freezing points that do not contain lithium. Numerous compositions listed in Table 2 contain no lithium and are relatively low-cost, low-freezing point mixtures that are likely to exhibit suitable physical properties. Salts containing enriched lithium will certainly have better neutronic performance than their analogs containing Na, Rb, or K, but at a significant extra expense associated with isotopic enrichment. If isotopically enriched materials are to be considered, then the boron-containing fluoroborate mixtures could be added to this list. The option of enriching boron for this particular application has never been proposed before, and there is no apparent basis for estimating the cost of enriching boron to the extreme levels required for this application (as was done for lithium). In addition to the issue of isotopic enrichment, an assessment of the BF₃ volatility in all of the fluoroborate salts will need to be considered. For the basis of property comparisons, fluoroborates are considered in a separate section of this report.

2.1.2 Vapor Pressure and Vapor Species

Most fluoride salts exhibit very low vapor pressures. Only compounds with higher oxidation state cations (such as BF_3 , UF_6 , and MoF_6) exhibit high vapor pressures. A few of the elements useful for coolants (BeF_2 , ZrF_4) exhibit appreciable vapor pressures (>1 mm Hg) at 800°C .

Table 3 catalogs the normal boiling and freezing points of single-component salts and of a few key multicomponent mixtures [10].

As is evident in Table 3, mixtures of these pure components will always exhibit lower vapor pressures (higher boiling points) than the most volatile constituent. Therefore, these salts do not exert significant vapor pressures (> 1 bar) except at very extreme temperatures. The MSRE operated with a cover pressure of 5 psig of helium, and the MSBR was designed for a cover pressure of 40 psig.

Table 3. Boiling and freezing points of salt compounds and key mixtures

Salt constituent(s)	Freezing point ($^\circ\text{C}$)	Normal boiling point ($^\circ\text{C}$)
LiF	845	1681
NaF	995	1704
KF	856	1502
RbF	775	1408
BeF_2	555	1327 ^a
ZrF_4	903	600 (sublimes)
LiF-NaF-KF (46.5-11.5-42)	454	1570
LiF- BeF_2 (67-33)	458	~ 1400 ^a
NaF- BeF_2 (57-43)	340	~ 1400 ^a
NaF- ZrF_4 (59.5-40.5)	500	~ 1350 ^a
RbF- ZrF_4 (58-42)	410	~ 1450 ^a

^aEstimated by extrapolation of lower-temperature data ($\sim 1100^\circ\text{C}$).

However, other factors are important. Even in a low-pressure system, the magnitude and nature of vapor produced from the salt needs to be evaluated. Experience with the ARE and the MSRE shows that very low salt vapor pressures (<1 mm Hg) simplify the off-gas system design and that certain vapor species can present problems.

In any high-temperature salt system, a purged cover gas will be necessary. The transport of significant amounts of salt vapor in this cover gas system can cause problems. In the operation of the ARE, it was found that the vapor over the ARE salt (53%NaF-41% ZrF₄-6%UF₄) was nearly pure ZrF₄. Because ZrF₄ sublimes rather than boils, ZrF₄ “snow” was found in the exhaust piping. The ZrF₄ was not returned to the salt reservoir by condensing as a liquid and draining back to the salt reservoir. Elaborate “snow traps” were designed (Fig. 7) to mitigate this problem [11], but it appears that a wise choice of salt composition can eliminate it completely.

The experience with the MSRE was quite different. The MSRE salts (65%LiF-29%BeF₂-5% ZrF₄-1% UF₄) exhibited very low vapor pressure, more than 100 times lower than the ARE salt. The vapor over the MSRE salt was also of a different character. This vapor contained both LiF and BeF₂ in a proportion that melted at a low temperature, such that the condensate would drain back to the reservoir as a liquid.

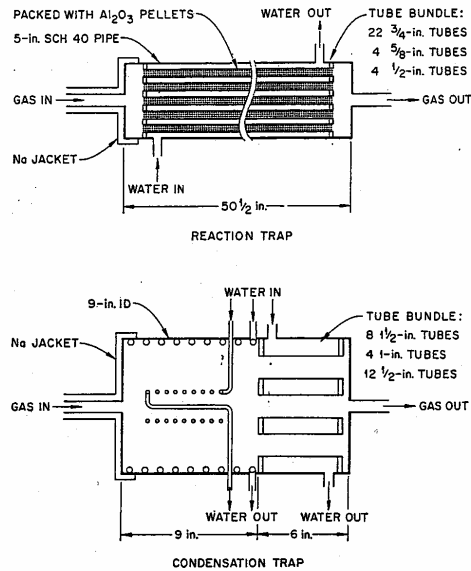


Fig. 7. ZrF₄ “snow-trap” designs developed for the Aircraft Reactor Test.

Vapor pressure is the physical property that is most sensitive to salt composition. Studies have been conducted to understand the effect of composition on the vapor pressure and vapor species of the thermodynamically non-ideal systems containing ZrF₄ and BeF₂ [12]. The results of these studies are useful for understanding and selecting the optimum coolant salt composition and are briefly reviewed in the following paragraphs.

The effect of salt composition on vapor pressure can be explained with the Lewis acid-base theory [13]. The native volatility of compounds containing the “acidic” constituent (Zr^{4+} , Be^{2+}) can be suppressed by donation of fluoride anions from the “basic” alkali fluoride constituent. The product of this donation is a low-volatility coordination-complex that is an integral part of the molten salt solution. Not all the alkali fluorides are equal in their ability to donate fluoride anions for coordination compounds. The affinity of alkali cations for their own fluoride anion decreases with increasing atomic number; thus, the heavier alkali elements will more readily donate their fluoride anions. Therefore, heavier alkali fluorides are more effective in reducing the native volatility of the compounds containing the acidic species (Zr^{4+} , Be^{2+}).

The effect of salt composition on vapor pressure is readily apparent in the BeF_2 and ZrF_4 systems. Figures 8 and 9 display the suppression of volatility as the ratio of alkali fluoride content increases so that it satisfies the coordination-bonding demands of the polyvalent cation. These figures also show the heavier alkali fluorides are more effective in suppressing the native volatility of the compound containing the polyvalent element (e.g., beryllium or zirconium).

The decrease of vapor pressure due to coordination bonding is also accompanied by a change in vapor composition. For a system rich in alkali fluoride, the vapor consists primarily of the alkali fluoride. For salt compositions that exist at the optimum ratio that just satisfies the coordination demands of the system, the vapor species is an association complex of the alkali fluoride and the polyvalent cation. For systems deficient in alkali fluoride, the volatile species is the parent compound containing the polyvalent cation. These trends are also indicated in Figures 8 and 9.

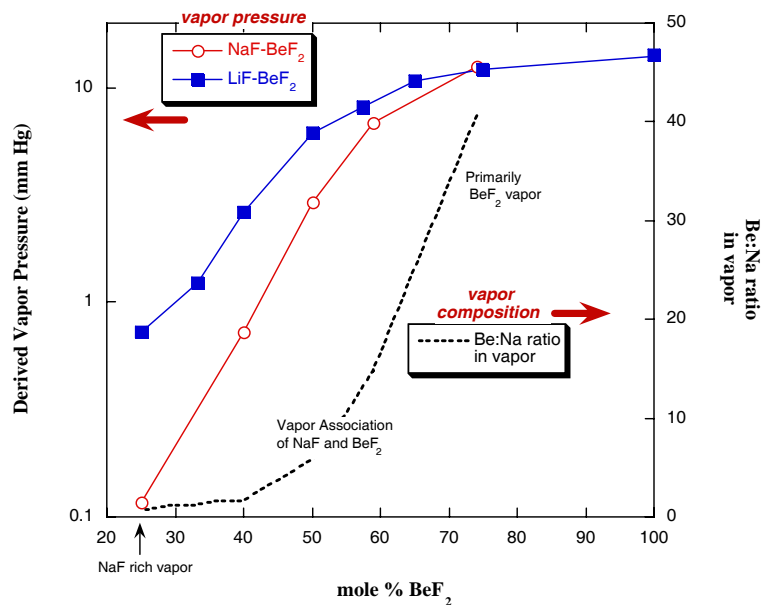


Fig. 8. Vapor pressure trends in alkali fluoride- BeF_2 systems at 900°C.

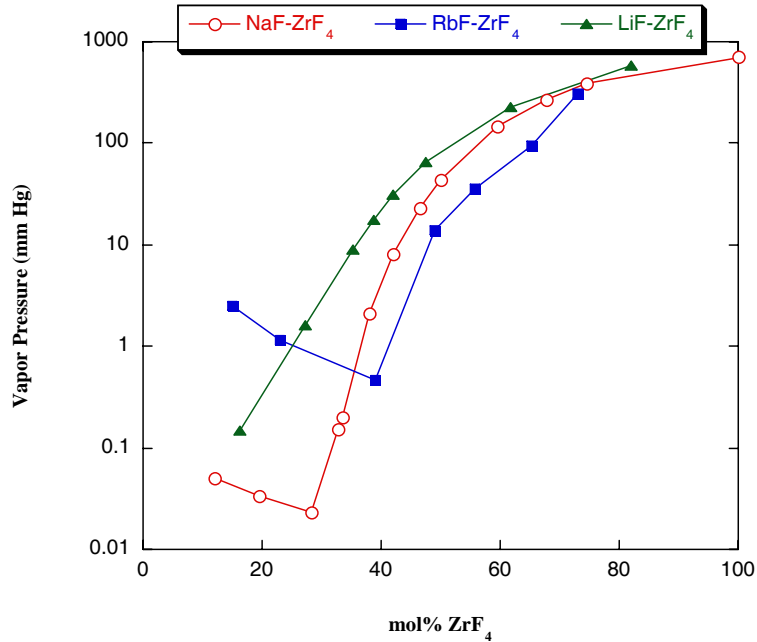


Fig. 9. Vapor pressure trends in alkali fluoride-ZrF₄ systems at 900°C.

From a practical standpoint, we should favor salt compositions with very low vapor pressures (<1 mm Hg at 900°C) that generate vapor species that readily melt after condensing. This corresponds to salt compositions with a ZrF₄ mole fraction in the range of ~20–45%, and with a mole fraction of BeF₂ less than ~35–45%, depending on the alkali cations present and the temperature under consideration.

2.1.3 Density

Fluid density is important for the purpose of gauging the heat transport capability of a coolant in both forced convection and (especially) natural convection. Density is among the most straightforward of properties to measure and is one of the most readily estimated for new compositions. Liquid salt density decreases linearly with increasing temperature. As expected, low atomic number salts tend to be light (sp.g. ~2) and high atomic number salts tend to be heavy (sp.g. > 4). Table 4 contains salt density equations developed from experimental measurements for some of the candidate AHTR salts [10].

Table 4. Salt density equations developed from experimental studies

Salt constituents	Molar composition	Density equation (g/cm ³)
LiF-BeF ₂	(66-34)	2.280-0.000488•T(°C)
NaF-BeF ₂	(57-43)	2.270-0.00037•T(°C)
LiF-BeF ₂ -ZrF ₄	(64.7-30.1-5.2)	2.539-0.00057•T(°C)
LiF-KF	(50-50)	2.460-0.00068•T(°C)
LiF-RbF	(43-57)	3.300-0.00096•T(°C)
LiF-NaF-KF	(46.5-11.5-42)	2.530-0.00073•T(°C)
NaF-ZrF ₄	(57-43)	3.650-0.00088•T(°C)

It was discovered that there is a simple and accurate method for predicting salt density based on additive molar volumes [14]. Oak Ridge National Laboratory (ORNL) researchers compiled a list of single-compound molar volumes, given in Table 5, that allows estimation of mixture densities to an accuracy better than 5% and permits useful density estimates for all of the AHTR candidate mixtures. The following relationship is recommended for prediction of molar volume and density for salt mixtures:

$$\rho_{\text{mix}}(T) = \frac{\sum X_i M_i}{\sum X_i V_i(T)} \quad (1)$$

where

- X_i = mole fraction of component i
- M_i = formula weight of component i (g/mole)
- $V_i(T)$ = molar volume of component i at temperature T

Values in Table 5 at two different temperatures allow interpolation or extrapolation to other temperatures.

Table 5. Standard molar volumes for use in estimation of mixture density

Component fluoride	Formula weight (g/mole)	Molar volume (cm ³ /mole)	
		600°C	800°C
⁷ LiF	26.0	13.46	14.19
NaF	42.0	19.08	20.20
KF	58.1	28.1	30.0
RbF	104.5	33.9	36.1
CsF	151.9	40.2	43.1
BeF ₂	47.0	23.6	24.4
MgF ₂	62.3	22.4	23.3
CaF ₂	78.1	27.5	28.3
AlF ₃	86.7	26.9	30.7
ZrF ₄	167.2	47.0	50.0

There is no a priori reason to select a salt based on density alone, except that salts that have a large density change with temperature may remove heat by natural convection better, resulting in better cooling. Very dense salts may develop undesirable hydrostatic heads and may make extra demands on pumping equipment, or may require consideration of buoyant graphite. Density will be factored into heat transfer metrics along with other fluid properties in Sect. 3. Density equations for candidate coolants not measured are listed in Table 6 according to the method of additive molar volumes.

Table 6. Salt density by method of additive molar volumes for candidate coolants not previously measured

Salt constituents	Molar composition	Density equation (g/cm ³)
LiF-NaF-RbF	42-6-52	$3.261-0.000811 \cdot T(^{\circ}\text{C})$
LiF-NaF-BeF ₂	31-31-38	$2.313-0.000450 \cdot T(^{\circ}\text{C})$
LiF-ZrF ₄	51-49	$3.739-0.000924 \cdot T(^{\circ}\text{C})$
RbF-ZrF ₄	58-42	$3.923-0.00100 \cdot T(^{\circ}\text{C})$
LiF-NaF-ZrF ₄	26-37-37	$3.533-0.000870 \cdot T(^{\circ}\text{C})$

2.1.4 Heat Capacity

Fluoride salts have relatively large heat capacities — in fact, they rival water in their ability to carry heat. The product of density and heat capacity is $\sim 1 \text{ cal/cm}^3\text{-}^\circ\text{C}$, the same value as for water. In the case of salts, the densities are somewhat greater than 1 g/cm^3 and the heat capacities are less than $1 \text{ cal/g-}^\circ\text{C}$, but the product is $\sim 1 \text{ cal/cm}^3\text{-}^\circ\text{C}$.

There is no fundamental theory that allows one to predict the heat capacity of various salt compositions, but the empirical method of Dulong and Petit, which assumes a contribution of $8 \text{ cal/}^\circ\text{C}$ per mole of each atom in the mixture, has been the most successful estimation method [14]. The Dulong and Petit estimation equation takes the form

$$C_p = 8 \cdot \sum X_i N_i / \sum X_i M_i, \quad (2)$$

where

X_i = mole fraction of component i

N_i = atoms per salt constituent i (g/mole) [= 2 for alkali halides, = 3 for BeF_2 , = 5 for ZrF_4]

M_i = formula weight of component i (g/mole)

This method is accurate to only $\pm 20\%$. Results for salts containing BeF_2 and ZrF_4 were more accurate ($\pm 10\%$) than those for the alkali fluorides. A measurement of the FLiNaK heat capacity in 1982 [15] gave the value as

$$C_p = 0.2333 + 2.54 \times 10^{-4} \cdot T[\text{K}] \text{ cal/g-}^\circ\text{C} . \quad (3)$$

This expression gives a heat capacity at 700°C of $0.48 \text{ cal/g-}^\circ\text{C}$, which is $\sim 7\%$ higher than the value measured at ORNL (0.45) in the 1950s [10]. Experimentally determined and estimated values of heat capacity are shown in Table 7. It should be noted that most of these experimental values were determined with relatively crude calorimeters as judged by today's standards. The experimental accuracy for these older measurements is no better than $\pm 10\%$. Modern calorimeters are capable of much more accurate measurements.

The measurement of the MSRE coolant salt (67%LiF-33% BeF_2) was refined and is more accurate (better than $\pm 2\%$) than the other values [16]. The variation of heat capacity with temperature is small and is typically neglected during preliminary calculations. The temperature variation was not resolved within the accuracy of most previous measurements.

Table 7. Experimental and estimated values of heat capacity for key salts

Salt components	Composition (mol %)	Heat capacity measured at 700°C (cal/g-°C)	Dulong-Petit prediction (cal/g-°C)
LiF-NaF-KF	46.5-11.5-42	0.45	0.387
LiF-KF	50-50	0.44	0.381
LiF-NaF-Rb	42-6-52	--	0.236
LiF-RbF	43-57	0.284	0.226
LiF-BeF ₂	66.7-33.3	0.577	0.566
NaF-BeF ₂	57-43	0.52	0.440
LiF-NaF-BeF ₂	31-31-38	--	0.489
LiF-ZrF ₄	51-49	--	0.292
Li-Na-ZrF ₄	26-37-37	--	0.296
NaF-ZrF ₄	57-43	0.28	0.275
KF-NaF-ZrF ₄	52-5-43	0.26	0.252
KF-ZrF ₄	58-42	--	0.251
RbF-ZrF ₄	58-42	--	0.200

2.2 FLUID TRANSPORT PROPERTIES

2.2.1 Viscosity

Molten salts exhibit normal fluid behavior. They are Newtonian fluids and exhibit the typical exponential decrease in viscosity, μ , with reciprocal temperature:

$$\mu \text{ (cP)} = A \exp (-B/T(\text{K})) . \quad (4)$$

Viscosity varies more with temperature than with any other fluid property. There are no truly predictive models for molten salt viscosity; therefore, viscosity has been measured for many systems by complementary methods. Even though there is a significant database, there are a number of important mixtures for which no information exists; therefore, it is necessary to examine the variation of viscosity with composition and to identify trends and bounds.

The information for binary mixtures is fairly complete and is displayed in Fig. 10 [10]. All of the three families of low-melting salts have mixtures that exhibit reasonably low viscosities (<10 cP) that make their use as industrial coolants possible. In contrast to other properties, compositional changes can have significant effects on fluid viscosity. These changes are evident in the variation of viscosity for different compositions within a binary or ternary system.

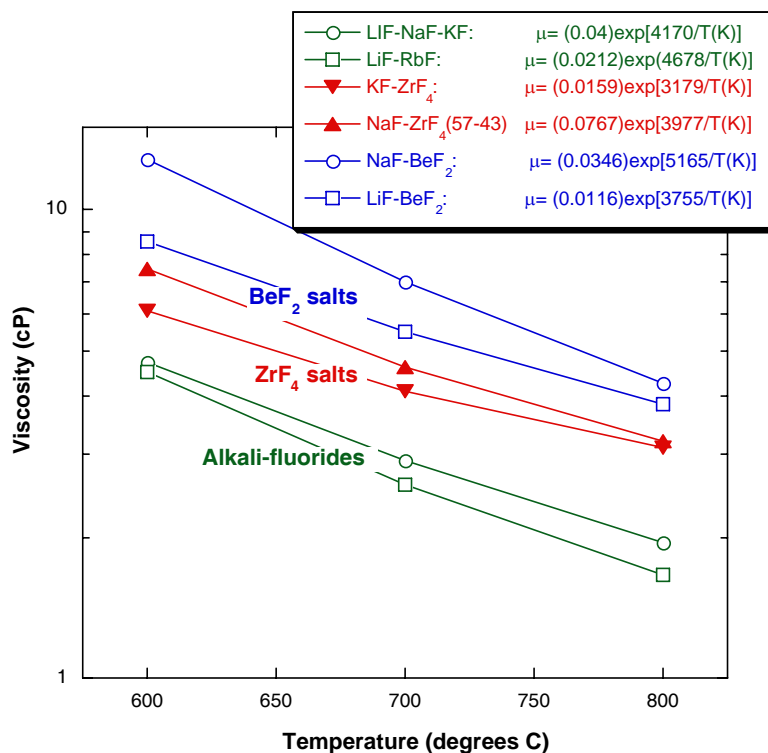


Fig. 10. Range of viscosities for various salt systems.

Viscosity, like vapor pressure and melting point, is strongly influenced by associative phenomena in the fluid phase. The influence of salt composition is most dramatic in the BeF₂ systems. The Be²⁺ cation has a special tendency to self-associate in fluoride melts that do not possess the requisite number of fluoride anions (1:4 Be:F) to satisfy the coordination demand of Be²⁺. The association of Be²⁺ cations leads to an extended network that acts to increase the viscosity of the molten salt. The thickening of the melt as the BeF₂ content increases (and the Be:F ratio in the entire melt decreases) is shown in Fig. 11 for LiF-BeF₂ [17] and in Fig. 12 for NaF-BeF₂ [18]. This thickening restricts the useful range of composition to less than 45% BeF₂. Figure 12 also reveals that the identity of the alkali cation in these systems has an effect. The more basic rubidium and sodium cations more readily donate the fluoride anion to Be²⁺ than does the lithium cation, resulting in a decreased amount of Be²⁺ self-association. Substitution of sodium for lithium, and rubidium for sodium or lithium, will lower the viscosity in these BeF₂ systems. The effect of potassium is expected to be intermediate between that of sodium and rubidium. Highly viscous pure BeF₂ was investigated to see whether it displayed non-Newtonian behavior. No deviation from Newtonian behavior was found [19].

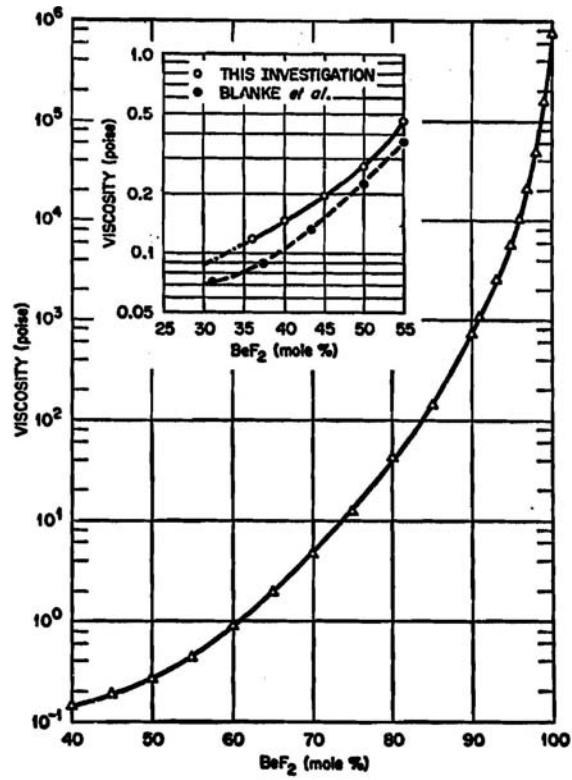


Fig. 11. Effect of BeF_2 composition on the viscosity of LiF-BeF_2 mixtures at 600°C .

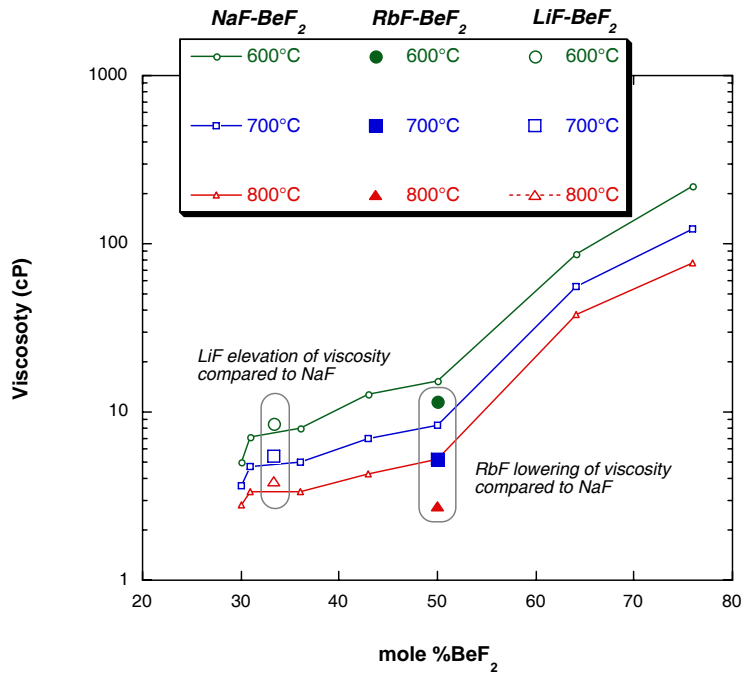


Fig. 12. Effect of alkali composition on the viscosity in BeF_2 salts.

It is more difficult to assess ZrF₄-salts in the same manner as BeF₂ salts [18]. The ZrF₄ phase diagrams have narrow low-melting regions; therefore, it is not possible to investigate large composition changes without also changing the alkali cation identity. Figure 13 displays the broadest low-melting phase field of NaF-ZrF₄ with a solid line. Within this range of ZrF₄ content (42 to 52%), the change in viscosity is not large, but it does increase slightly with increasing ZrF₄ content. The effect of adding or replacing the alkali cation is the same in the BeF₂ system: lighter alkalis increase the viscosity, and heavier alkalis reduce the viscosity.

The variation in viscosity of various alkali fluoride mixtures is not large (Fig. 10) and follows the same basic trend found for the BeF₂ and ZrF₄ systems. Heavier alkali mixtures are less viscous than lighter alkali systems.

It should also be noted that the three families of salts represent three distinct classes of liquid behavior. The alkali fluorides are ideal mixtures of very similar chemical constituents with very little associative behavior, whereas both ZrF₄ and BeF₂ mixtures are potential glass-formers [20]. BeF₂-rich mixtures are “strong” glass formers characterized by extended association of cations into networks of large extent, thus giving rise to high viscosity “glassy” mixtures. BeF₂ is the fluoride analog to the SiO₂ glasses. Mixtures of ZrF₄ and alkali halides represent a different class of “fragile” glass mixtures that form due to a particular type of mixture thermodynamics that inhibits crystallization and preserves an amorphous structure during the liquid/solid phase transition. The ZBLA (ZrF₄-BaF₂-LaF₃) and ZBLAN (ZrF₄-BaF₂-LaF₃-NaF) glasses used for infrared optics are examples of this type of fragile glass [21]. These types of fragile glasses are different than network glasses in that the glass-forming compositions are relatively low-viscosity fluids rather than high-viscosity fluids [18].

The accuracy of previous viscosity determinations can be assessed by comparing the early ORNL measurements conducted during the 1950s and 1960s and the few recent investigations [22–23]. These comparisons can be made for systems of alkali fluorides and ZrF₄-mixtures and are shown in Figs. 14 and 15. The deviation between the older and newer measurements is about 10%, with the older measurements predicting higher values. The older ORNL values are based on agreement of measurements obtained from capillary efflux and rotational viscometers. The newer measurements were obtained from a novel oscillating cup viscometer customized for high temperatures and sensitive to low-viscosity fluids. This agreement between newer and older values is within the error band reported for the older measurements ($\pm 20\%$). For more sophisticated viscosity correlations and extrapolation to higher temperatures, the methods recommended by Veliyulin [24] can be used.

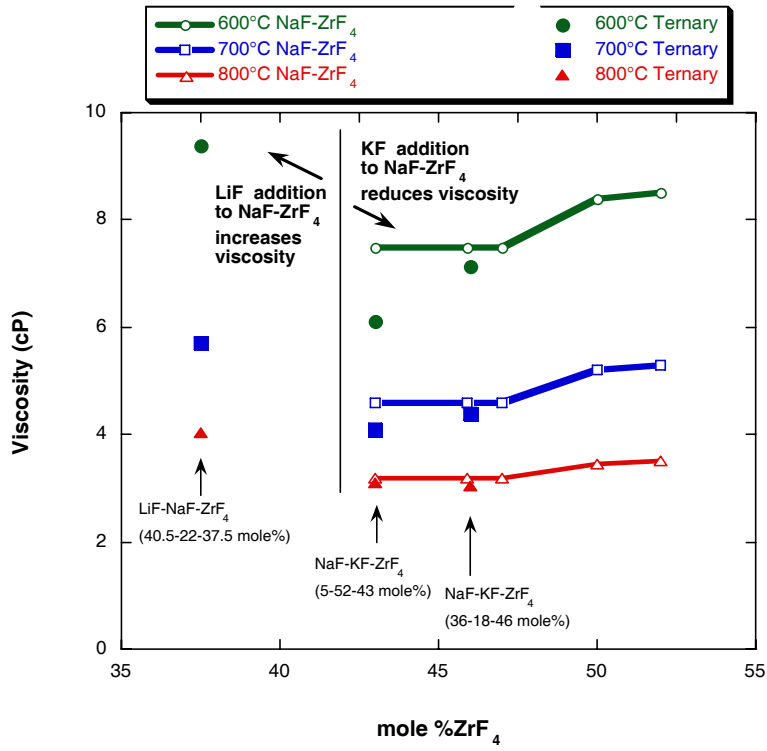


Fig. 13. Composition effects on viscosity in ZrF₄ mixtures

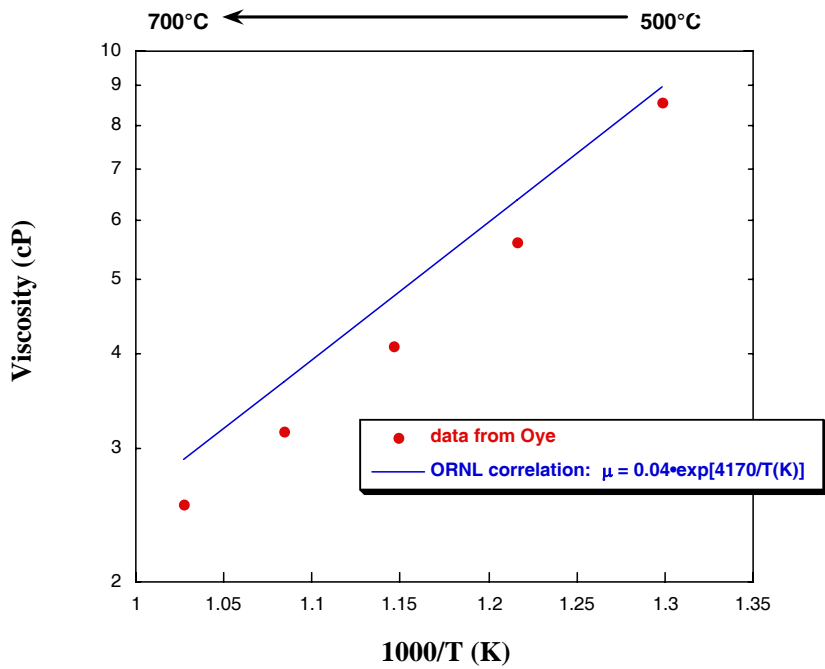


Fig. 14. Comparison of values measured for the viscosity of LiF-NaF-KF eutectic.

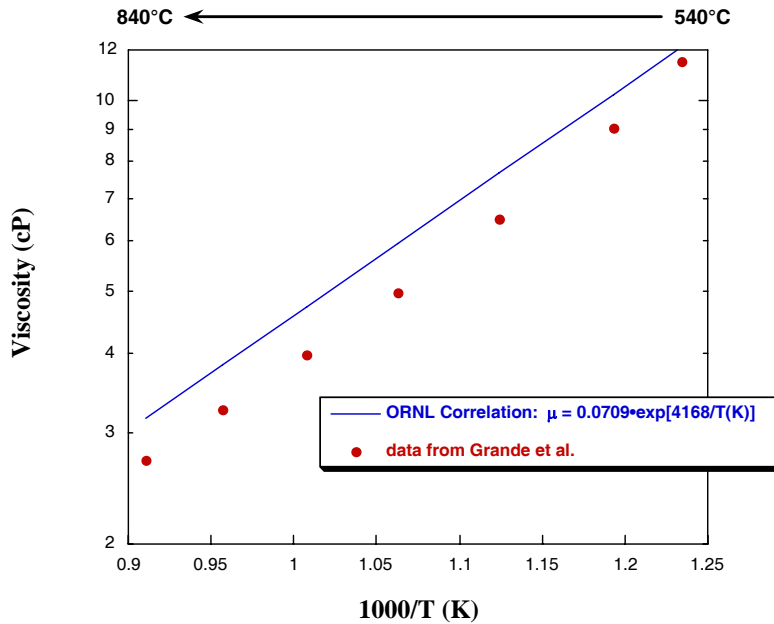


Fig. 15. Comparison of values measured for the viscosity of NaF-ZrF₄, 50-50 mol %.

2.2.2 Thermal Conductivity

The thermal conductivity of molten salt is the most difficult fluid property to measure, and it has led to the greatest amount of confusion and error in heat-transfer calculations. This state of affairs is reflected in the general scientific literature on molten salt conductivity [25–27] and in the work focused on molten salt reactors [28–30]. In early studies at ORNL using a variable-gap apparatus, conductivities were reported that were four times higher than the value now believed to be correct [18]. An improved variable-gap apparatus was designed to minimize the errors due to convection and bypassing heat flow [29]. A far lower thermal conductivity was measured with the improved apparatus, and these results were more similar to the values found for other salt systems using hot-wire and annular cylinder techniques [30].

These errors in the measurement of thermal conductivity led to a number of erroneous conclusions [31]. All of the systematic errors in measurement led to higher apparent values for thermal conductivity. When heat-transfer studies were conducted using the “high” value for thermal conductivity, it was found that the heat flow was lower than expected based on universal correlations for convective heat transfer. Because of the unexpected “low” heat flux, it was postulated that a significant film resistance must exist, and it was assumed that some type of insulating film impeded heat flow between the salt and the metal. A film coefficient was assumed in order to correct for this apparent discrepancy—but the discrepancy actually resulted from an

error in calculating the thermal conductivity of the salt. Numerous corrosion studies on alloys exposed to salt for many years show that there is no such film on the surface of metals and that there is no heat-transfer impediment due to insulating films. Fluoride salts are excellent fluxes for both oxides and fluorides and quickly dissolve corrosion products. Metallic corrosion products are dissolved in the salt solution. It was also found that “the overall heat transfer coefficient of the MSRE heat exchanger did not change during 22,000 h of salt circulation and 13,000 equivalent full-power hours of operation, thus indicating no buildup of scale and no evidence of gas filming” [32]. Detailed forced-convection heat-transfer measurements confirmed this same behavior in out-of-pile tests with the MSBR fuel salt composition [33].

The high values for the measured conductivity also caused confusion in the modeling and correlation of molten salt conductivity. To account for the high values of measured conductivity, Gambill [34] proposed that molten salts contribute to conductivity due to a diffusional mechanism, in addition to the normal vibrational mechanism. Later studies showed that the primary mechanism for heat transfer is from vibrational modes; therefore, molten salts have conductivities in the same range as solid dielectrics [25].

Because measurement of high-temperature fluid thermal conductivity is a difficult task with a number of potential sources of error, considerable scatter exists in the experimental database. However, if the most reliable results using the hot-wire and annular cylinder methods are compared, the results are more consistent and are amenable to modeling. The most successful model for predicting the thermal conductivity of molten salts was proposed by Rao and refined by Turnbull [25]:

$$k \text{ (watt/m-K)} = 0.119 \cdot T_m^{0.5} \cdot \rho^{0.667} / (M/n)^{1.167}, \quad (5)$$

where

- T_m = melting point (K)
- ρ = molar volume of the molten salt at (cm^3/mole)
- M = average formula weight of the salt ($= \sum X_i M_i$)
- n = the number of discrete ions per salt formula ($= 2$ for simple salts like NaCl)

This model was originally proposed for simple one-component salts such as NaCl, but has been extended to mixtures with polyvalent cations. Mixtures of salt components are expected to exhibit a thermal conductivity slightly below the mole-fraction weighted average of the single components due to disruption of the vibrational modes of the quasi-crystalline lattice. The application of this model to salts with polyvalent cations requires an assignment of the ion-number n , based upon some assumption for speciation. Both of these factors introduce some uncertainty in the predictions for more complex salt systems. For all of the estimates below it has been assumed that $n = 2$.

Ignatiev and Khoklov [35,38] recommend an empirical equation that is simply a function of temperature (T) and salt formula weight (M) for correlating thermal conductivity:

$$k \text{ (watt/m-K)} = 0.0005 \cdot T(\text{K}) + 32.0/M - 0.34 . \quad (6)$$

The database for the Russian correlation includes a large number of alkali halides, BeF₂-salts, and salts containing UF₄ and ThF₄. Table 8 presents the measured thermal conductivity values for halide salts that are expected to be the most reliable and the results of both predictive methods. The trend of decreasing thermal conductivity with increasing formula weight of the salt has been found in other measurements on pure halide salts and their mixtures [25, 36–38]. There are almost no reliable data on the thermal conductivity of ZrF₄-containing salts.

Table 8. Comparison of measured and predicted thermal conductivities

Salt composition (mol %)	Formula weight (g/mole)	Melting point (°C)	Temp (°C)	Measured ^a conductivity (watt/m-K)	Rao-Turnbull prediction (watt/m-K)	Kokhlov correlation (watt/m-K)
LiCl-KCl (56-41)	55.6	355	355	0.69	0.65	--
LiF-NaF-KF (46.5-11.5-42)	41.3	454	500 700	0.60	0.68	0.82 0.92
LiF-NaF-RbF (42-6-52)	67.8	435	700	--	0.42	0.62
LiF-BeF ₂ (66.7-33.3)	33.0	460	600	1.0	0.79	1.1
NaF-BeF ₂ (57-43)	44.1	340	700	--	0.58	0.87
LiF-NaF-BeF ₂ (26-37-37)	38.9	315	700	--	0.62	0.97
LiF-ZrF ₄ (51-49)	95.2	509	700	--	0.35	0.48
NaF-ZrF ₄ (59.5-40.5)	92.7	500	700	--	0.36	0.49
KF-ZrF ₄ (58-42)	103.9	390	700	--	0.32	0.45
RbF-ZrF ₄ (58-42)	130.8	410	700	--	0.26	0.39
LiF-NaF-ZrF ₄ (26-37-37)	84.16	436	700	--	0.36	0.53
NaF-AlF ₃ (75-25)	52.5	1000	1000	0.80	0.79	0.91

^aMeasured values are drawn from Refs. 13, 16, 21, and 22.

3. HEAT-TRANSFER COMPARISONS

It is useful to compare the heat-transfer performance of the AHTR candidate coolants to other coolants with which we have experience, or would like to consider for related applications (secondary heat transfer fluids). With the exception of water, the temperature of 700°C was selected for comparison because this permits properties to be evaluated more readily. A temperature of 300°C was selected for water, because this is a typical coolant temperature used in the primary circuit of existing nuclear power plants.

Table 9 lists the properties of the coolants to be used in the heat-transfer comparisons, as well as the properties of ten candidate AHTR salts.

Table 9. Properties of comparison coolants and candidate coolants at 700°C

Coolants	Heat capacity, C_p (cal/g-°C)	Density, ρ (g/cc)	Viscosity, μ (cP)	Volume expansivity, β (1/°C)	Thermal conductivity, k (W/m-K)	Prandtl # $C_p \cdot \mu / k$
<i>Comparison coolants</i>						
Water(300°C)	1.370	0.72	0.09	3.30E-03	0.54	0.967
Na (550°C)	0.303	0.82	0.23	8.60E-04	62	0.004
NaF-NaBF ₄ (700°C)	0.360	1.75	0.88	4.25E-04	0.5	2.640
<i>Candidate salt coolants at 700°C</i>						
FLiNaK	0.450	2.02	2.9	3.61E-04	0.92	5.938
LiF-NaF-RbF	0.236	2.69	2.6	3.01E-04	0.62	4.143
2LiF-BeF ₂	0.577	1.94	5.6	2.52E-04	1	13.525
NaF-BeF ₂	0.520	2.01	7	1.84E-04	0.87	17.513
LiF-NaF-BeF ₂	0.489	2.00	5	2.25E-04	0.97	10.551
LiF-ZrF ₄	0.292	3.09	> 5.2	2.99E-04	0.48	> 13.241
NaF-ZrF ₄	0.280	3.14	5.1	2.96E-04	0.49	12.199
KF-ZrF ₄	0.251	2.80	< 5.1	3.17E-04	0.45	< 11.907
RbF-ZrF ₄	0.200	3.22	5.1	3.11E-04	0.39	10.948
LiF-NaF-ZrF ₄ ^a	0.300	2.79	6.9	3.12E-04	0.53	19.073

^a For 26-37-37 mol %.

Generalized heat-transfer metrics are a useful tool for grouping coolant performance in the absence of more detailed system designs. Bonilla [39] has provided general figures of merit (FOM) based on minimal pumping power for a given coolant temperature rise as the objective function for forced convection:

$$\text{FOM (forced convection, turbulent)} = \mu^{0.2} / (\rho^2 C_p^{2.8}), \quad (7)$$

where

$$\begin{aligned}\mu &= \text{viscosity} \\ \rho &= \text{fluid density} \\ C_p &= \text{heat capacity}\end{aligned}$$

For natural convection cooling, Bonilla also provide the following groups for passive cooling:

$$\text{FOM (natural convection, turbulent)} = [\mu^{0.2} / \beta \rho^2 C_p^{1.8}]^{0.36} \quad (8)$$

$$\text{FOM (natural convection, laminar)} = [\mu / \beta \rho^2 C_p]^{0.5} \quad (9)$$

where

$$\beta = \text{volume expansivity} = 1/\rho \cdot d\rho/dT [1/^\circ\text{C}] .$$

During evaluation of secondary coolants for the MSBR, Sanders [5] proposed a FOM related to the area required for the primary heat exchanger:

$$\text{FOM (heat exchanger area)} = \mu^{0.2} / [C_p^{0.6} k^{0.6} \rho^{0.3}] . \quad (10)$$

Sanders recommends that this FOM be used only for comparison within a coolant group type (salts, metals, or other). All of these FOMs are “golf-scores” — i.e., lower numbers correlate with better performance. Tables 10 and 11 summarize the various FOMs for the comparison of candidate coolants.

In general, we can conclude that the lighter molten salts (those *not* containing large quantities of higher-atomic-number elements, e.g., rubidium and zirconium) have somewhat better heat transfer performance than the heavy salts. The one exception is the laminar regime of natural convection. In most passive cooling situations, the turbulent natural convection component is of primary importance.

Table 10. Turbulent convection and heat exchanger area figures of merit

Turbulent forced convection		Heat exchanger area	
Coolant	Figure of merit ^a	Coolant	Figure of merit ^a
Water (300°C)	0.20	Na	1.6
LiF-BeF ₂	0.70	Water (300°C)	13.0
NaF-BeF ₂	0.91	LiF-BeF ₂	21.5
LiF-NaF-BeF ₂	1.02	FLiNaK	21.6
FLiNaK	1.13	LiF-NaF-BeF ₂	22.6
LiF-NaF-ZrF ₄ ^b	1.42	NaF-BeF ₂	25.2
LiF-ZrF ₄	1.82	NaF-NaBF ₄	28.0
NaF-ZrF ₄	1.98	LiF-NaF-RbF	31.8
NaF-NaBF ₄	2.20	LiF-NaF-ZrF ₄	35.9
KF-ZrF ₄	3.39	NaF-ZrF ₄	37.4
LiF-NaF-RbF	3.79	LiF-ZrF ₄	37.5
RbF-ZrF ₄	4.82	KF-ZrF ₄	42.5
Na	13.15	RbF-ZrF ₄	48.7

^aSuperior ranking is indicated by lower values

^bFor 26-37-37 mol %.

Table 11. Natural convection figures of merit

Turbulent natural convection		Laminar natural convection	
Coolant	Figure of merit ^a	Coolant	Figure of merit ^a
Water (300°C)	4.8	Water (300°C)	0.63
FLiNaK	13.3	Na	3.60
LiF-BeF ₂	13.9	NaF-NaBF ₄	4.31
LiF-NaF-ZrF ₄ ^b	13.9	FLiNaK	6.61
LiF-ZrF ₄	14.5	LiF-NaF-RbF	7.11
NaF-NaBF ₄	14.7	LiF-ZrF ₄	7.90
NaF-ZrF ₄	14.7	NaF-ZrF ₄	7.90
LiF-NaF-BeF ₂	15.6	RbF-ZrF ₄	8.89
NaF-BeF ₂	16.5	LiF-NaF-ZrF ₄ ^b	9.01
KF-ZrF ₄	16.7	KF-ZrF ₄	9.05
LiF-NaF-RbF	17.4	2LiF-BeF ₂	10.12
RbF-ZrF ₄	17.6	LiF-NaF-BeF ₂	10.66
Na	20.0	NaF-BeF ₂	13.45

^aSuperior ranking is indicated by lower values

^bFor 26-37-37 mol %.

4. NUCLEAR PROPERTIES

An assessment of the neutronics properties for several coolant options was performed to evaluate the effect of various salts on the standard operating conditions of the reactor and the long- and short-term effects of neutron activation of the primary salts.

4.1 PARASITIC NEUTRON CAPTURE AND MODERATION

The thermal-spectrum AHTR reactor core design consists of three major constituents: the fuel, the moderator, and the coolant. The purpose of the moderator (graphite) is to reduce the energy of neutrons so that they will be easily absorbed in the fuel to cause additional fissions. Any neutrons that are captured and fail to generate a fission reaction are considered parasitic to the critical chain reaction in the core. Graphite has a very small probability of capturing neutrons; therefore, the major component of parasitic neutron capture is the liquid-salt coolant. The parasitic-neutron-capture rate is directly related to the efficiency of fuel utilization: increased parasitic neutron capture requires additional fuel to maintain a critical system. If the coolant also moderates neutrons, this benefit can offset the parasitic capture.

The relationship between capture and moderation is especially significant during a theoretical accident scenario, when all or part of the coolant could be displaced with a void, such as boiled coolant, a gas bubble trapped in the system, a blocked coolant channel, or a breach of the reactor vessel. In these “beyond-design-basis” accident scenarios, the increase in reactivity should be minimized (preferably, there should be a decrease) when the void displaces the coolant.

Table 12 displays the parasitic-neutron-capture rates (relative to pure graphite on a per-unit-volume basis) for the candidate salts from Table 2. The table also displays the moderating ratio, a FOM that relates the effectiveness of moderation versus the parasitic neutron capture for a given energy range:

$$\text{Moderating Ratio} = \frac{\xi \Sigma_s \phi(\Delta E)}{\Sigma_c \phi(\Delta E)}, \quad (11)$$

where

$$\begin{aligned} \xi \Sigma_s \phi(\Delta E) &= \text{rate of energy loss (lethargy gain) due to neutron scattering for a} \\ &\text{given energy range} \\ \Sigma_c \phi(\Delta E) &= \text{rate of parasitic neutron capture for the same energy range} \\ \Delta E &= 0.1 \text{ to } 10 \text{ eV for this analysis .} \end{aligned}$$

Table 12. Neutronic efficiency for comparison materials and candidate coolants^a

Material	Total neutron capture (per unit volume) relative to graphite	Moderating ratio (avg. over 0.1–10 eV)
Heavy water	0.2	11449
Light water	75	246
Graphite	1	863
Sodium	47	2
UCO	285	2
UO ₂	3583	0.1
LiF-BeF ₂	8	60
LiF-BeF ₂ -ZrF ₄	8	54
NaF-BeF ₂	28	15
LiF-BeF ₂ -NaF	20	22
LiF-ZrF ₄	9	29
NaF-ZrF ₄	24	10
LiF-NaF-ZrF ₄ ^b	20	13
KF-ZrF ₄	67	3
RbF-ZrF ₄	14	13
LiF-KF	97	2
LiF-RbF	19	9
LiF-NaF-KF	90	2
LiF-NaF-RbF	20	8

^aComputations conducted with 99.995 ⁷Li

^bFor 42-29-29 mol %.

As indicated in Table 12, the total neutron capture of light water (H₂O) is very large, much larger than that of the other traditional coolants, such as heavy water (D₂O) or graphite, and also larger than that of most of the salts. However, the excellent moderating power of light water leads to a much larger moderating ratio than that of any salt coolant. The neutron-capture rates of the salts are much larger than those of (pure) graphite; therefore, minimizing the coolant in the core will improve the fuel efficiency substantially from a neutronics perspective.

The BeF₂ salts have the best neutronics properties (large moderating ratios and small parasitic capture rates), while the alkali fluorides have the worst. The salts with low moderating ratios can be expected to have the highest increase in reactivity when a void displaces coolant.

The results in Table 12 were produced in a pin-cell calculation using the TRITON/NEWT depletion sequence with the CENTRM resonance processing tool from SCALE5.1, with a 238-group ENDF/B-VI cross-section set. The ⁷Li enrichment is 99.995% in the LiF constituent.

4.2 REACTIVITY COEFFICIENTS

The thermal-spectrum Liquid-Salt-Cooled Very High-Temperature Reactor (LS-VHTR or AHTR) core consists of three constituents: TRISO fuel, graphite-moderator, and molten-salt coolant. A distinct feature of the liquid-salt cooled version of the Very High-Temperature Reactor (VHTR) is that a major component of parasitic neutron capture, and a significant amount of moderation, can reside in the liquid-salt coolant. The relationship between capture and moderation is especially significant during transients or accident conditions; for example, when coolant is removed from the core by a temperature-driven density change, a coolant void is postulated, a gas bubble is trapped in the system, or a breach of the primary circuit occurs. For these scenarios, the increase in reactivity due to coolant-density reduction should be minimized or mitigated when the transient or accident occurs.

A prismatic VHTR system was chosen to evaluate these scenarios. The standard hexagonal fuel-block consists of TRISO particle fuel (25% packing fraction, 15% enriched), a 1.27-cm-diam. fuel channel, 108 coolant channels, and 216 fuel channels. Because of the superior heat-transfer properties of the salt compared to those of helium, the coolant channels were reduced to 0.935 cm in diameter (7% of the block volume). The results for this study were produced from a pin-cell calculation using the TRITON/NEWT depletion sequence with CENTRM resonance-processing tool from SCALE5.1, with a 238-group ENDF/B-IV cross-section set. AHTR salt coolants were analyzed with the TRITON lattice physics sequence within SCALE. A ${}^7\text{Li}$ enrichment of 99.995% was used for lithium-containing coolants (unless noted otherwise). More detailed documentation of this model is available in a recent report [40].

Table 13 displays the coolant density coefficient (reactivity change due to coolant expansion on heating) and the coolant void ratio (CVR), which is the change in reactivity due to a 100% voiding scenario, for a variety of salt coolants in the AHTR design with Er_2O_3 poison. All salts except $\text{LiF}\text{-BeF}_2$ contribute a positive coolant density coefficient and CVR. Positive voiding or coolant density coefficients are often characterized as “forbidden” zones for reactors, but it is important to look at the entire reactivity response of the core before passing judgment on the reactor response.

Table 13. Reactivity coefficients for coolant loss

Salt	Composition (mol %)	Coolant density coefficient (Dollars per 100°C)	Coolant void ratio (Dollars)
LiF-BeF ₂	67-33	-\$0.01	-\$0.11
LiF-ZrF ₄	51-49	\$0.04	\$1.40
NaF-BeF ₂	57-43	\$0.06	\$2.45
LiF-NaF-ZrF ₄	42-29-29	\$0.06	\$2.04
LiF-NaF-ZrF ₄	26-37-37	\$0.09	\$2.89
NaF-ZrF ₄	59.5-40.5	\$0.11	\$3.44
NaF-RbF-ZrF ₄	33-23.5-43.5	\$0.15	\$4.91
RbF-ZrF ₄	58-42	\$0.18	\$6.10
KF-ZrF ₄	58-42	\$0.27	\$7.92

It is necessary to consider that the AHTR is a pool-type reactor operating at near-atmospheric pressure with a margin to boiling for the coolant of $\sim 500^\circ\text{C}$. Thus there can be no depressurization, which leads to a sudden loss of coolant. Off-normal conditions that result in a decrease of coolant in the core are either caused, or accompanied by, a temperature change. Therefore, the total temperature coefficient should also be considered in the choice of salt coolant. A loss of forced circulation (e.g., break in a major coolant pipe) will result in an increased coolant temperature, but note that the fuel temperature also will rise more quickly. A sudden reactivity insertion will cause a rise in coolant temperature, but this rise will lag behind the rapid rise in fuel temperature. Therefore, the relative magnitude and sign of the coolant temperature plus the coolant density coefficient (or total coolant temperature coefficient) should be considered with respect to the total noncoolant (fuel plus graphite) temperature coefficient.

Table 14 shows a group of temperature coefficients for an AHTR fuel block for conditions with and without Er_2O_3 poison. The total coolant temperature coefficient is far smaller than the noncoolant negative temperature coefficient. This effect is more pronounced when erbium poison is added to the core because a small change in temperature substantially increases the fraction of neutrons in the 0.3 eV resonance of ^{167}Er .

Therefore, if the possibility of a complete voiding without a temperature change can be removed from consideration (as is assumed with liquid-metal fast reactors), the significance of a coolant density change must be considered with respect to all other temperature coefficients. For any scenario driven by a rapid reactivity insertion, coolants that exhibit small negative temperature coefficients do not control the system response because the total response is dominated by the negative reactivity effects in the closely coupled fuel. However, for salt

Table 14. Reactivity coefficients for AHTR with 900°C inlet

Salt	Composition mol %	Coefficients of reactivity (Dollars per 100°C)					
		Coolant			Noncoolant		
		Temp	Density	Total	Fuel	Graphite	Total
<i>Coefficients without Er₂O₃ poison present</i>							
LiF-BeF ₂	67-33	-\$0.01	\$0.01	\$0.00	-\$0.46	-\$0.12	-\$0.58
LiF-ZrF ₄	51-49	-\$0.01	\$0.04	\$0.03	-\$0.64	\$0.03	-\$0.61
NaF-BeF ₂	57-43	\$0.00	\$0.06	\$0.07	-\$0.41	\$0.02	-\$0.39
LiF-NaF-ZrF ₄	42-29-29	-\$0.01	\$0.06	\$0.05	-\$0.47	-\$0.03	-\$0.50
LiF-NaF-ZrF ₄	26-37-37	\$0.00	\$0.09	\$0.09	-\$0.41	\$0.00	-\$0.41
NaF-ZrF ₄	59.5-40.5	\$0.00	\$0.11	\$0.11	-\$0.39	\$0.05	-\$0.35
NaF-RbF-ZrF ₄	33-23.5-43.5	\$0.00	\$0.14	\$0.13	-\$0.37	\$0.12	-\$0.25
RbF-ZrF ₄	58-42	-\$0.02	\$0.17	\$0.15	-\$0.50	\$0.07	-\$0.43
KF-ZrF ₄	58-42	-\$0.01	\$0.27	\$0.26	-\$0.57	\$0.05	-\$0.52
<i>Coefficients with Er₂O₃ poison present</i>							
LiF-BeF ₂	67-33	-\$0.09	\$0.00	-\$0.09	-\$0.92	-\$1.54	-\$2.45
LiF-ZrF ₄	51-49	-\$0.03	\$0.04	\$0.01	-\$0.64	-\$1.42	-\$2.08
NaF-BeF ₂	57-43	-\$0.08	\$0.06	-\$0.01	-\$0.86	-\$1.40	-\$2.25
LiF-NaF-ZrF ₄	42-29-29	-\$0.03	\$0.06	\$0.03	-\$0.47	-\$1.38	-\$1.85
LiF-NaF-ZrF ₄	26-37-37	-\$0.05	\$0.09	\$0.04	-\$0.87	-\$1.41	-\$2.27
NaF-ZrF ₄	59.5-40.5	-\$0.05	\$0.11	\$0.06	-\$0.85	-\$1.37	-\$2.21
NaF-RbF-ZrF ₄	33-23.5-43.5	-\$0.05	\$0.15	\$0.11	-\$0.82	-\$1.29	-\$2.10
RbF-ZrF ₄	58-42	-\$0.04	\$0.19	\$0.15	-\$0.50	-\$1.31	-\$1.81
KF-ZrF ₄	58-42	-\$0.02	\$0.27	\$0.25	-\$0.57	-\$1.33	-\$1.90

^aComputations conducted with 99.995 ⁷Li

coolants with a positive total coolant temperature coefficient, a coupled neutronics/thermal-hydraulics analysis (e.g., PARCS or NESTLE coupled with RELAP) must be performed to understand the net reactivity effect. In this regard, it is useful to define a new parameter, the coolant safety ratio, which is the ratio of the magnitude of a positive (total) coolant temperature coefficient and the total noncoolant temperature coefficient. For instance, a coolant safety ratio of 1.9% implies that the fuel and graphite must increase only 1.9°C to offset a 100°C increase in coolant temperature.

These safety-related parameters for the leading coolant candidates are shown in Table 15. The design basis for the AHTR includes a two-batch core with a 1.5-year cycle and a burnup of 150 MWd/kgU. Therefore, because of differences in parasitic capture of the salt, the enrichment levels were varied to reach these design specifications. The following parameters were varied in our calculations in order to explore the effects on reactivity coefficients: (a) coolant volume

Table 15. Effect of key core design parameters on AHTR reactivity coefficients^a

Salt	Composition (mol %)	²³⁵ U enrichment (wt %)	Coolant void ratio (Dollars)	Total coolant coefficient (Dollars per 100°C)	Salt coolant safety ratio (%)	Total thermal coefficient (Dollars per 100°C)
<i>Coefficients without Er₂O₃ poison, 7% coolant fraction</i>						
LiF-BeF ₂	67-33	14.1	\$0.28	\$0.00	-0.1%	-\$0.58
NaF-BeF ₂	57-43	15.4	\$2.71	\$0.07	17.0%	-\$0.32
LiF-NaF-ZrF ₄	26-37-37	15.5	\$2.83	\$0.09	21.5%	-\$0.32
NaF-ZrF ₄	59.5-40.5	15.8	\$3.35	\$0.11	30.5%	-\$0.24
NaF-RbF-ZrF ₄	33-23.5-43.5	16.5	\$4.39	\$0.13	53.8%	-\$0.11
<i>Coefficients with Er₂O₃ poison, 7% coolant fraction</i>						
LiF-BeF ₂	67-33	14.3	-\$0.11	-\$0.09	-3.7%	-\$2.54
NaF-BeF ₂	57-43	15.6	\$2.45	-\$0.01	-0.6%	-\$2.26
LiF-NaF-ZrF ₄	26-37-37	15.8	\$2.89	\$0.04	1.9%	-\$2.23
NaF-ZrF ₄	59.5-40.5	16.1	\$3.44	\$0.06	2.9%	-\$2.14
NaF-RbF-ZrF ₄	33-23.5-43.5	16.9	\$4.91	\$0.11	5.1%	-\$2.00
<i>Coefficients with Er₂O₃ poison, 7% coolant fraction, 99.9% ⁷Li</i>						
LiF-BeF ₂	67-33	19.2	\$9.56	\$0.17	9.4%	-\$1.62
LiF-NaF-ZrF ₄	26-37-37	16.9	\$4.99	\$0.12	5.1%	-\$2.16
<i>Coefficients with Er₂O₃ poison, 15% coolant fraction</i>						
LiF-BeF ₂	67-33	15.5	-\$0.64	-\$0.19	-8.8%	-\$2.40
NaF-BeF ₂	57-43	18.0	\$4.63	-\$0.04	-2.2%	-\$1.81
LiF-NaF-ZrF ₄	26-37-37	18.7	\$5.83	\$0.08	4.2%	-\$1.78
NaF-ZrF ₄	59.5-40.5	19.3	\$6.98	\$0.12	7.2%	-\$1.57
NaF-RbF-ZrF ₄	33-23.5-43.5	21.2	\$10.41	\$0.21	15.0%	-\$1.21

^aAll calculations performed with 99.995 % ⁷Li unless noted

fraction (7%, 15%); (b) Er₂O₃ poison level in the fuel-compact matrix (0, 5 mg/cm³); and (c) ⁷Li enrichment level (99.995, 99.9). The calculations were also performed with the simplifying assumption that the temperature rise was uniformly distributed over all materials in the core (fuel-coolant-moderator). This assumption is likely to cause an exaggeration of the positive reactivity contributions arising from the salt coolant.

A careful comparison of the results in Table 15 reveals that the reactivity coefficients that affect safety, other than CVR, depend more on the coolant fraction and poison content than the choice of salt coolant. Therefore, each of the salt-coolant options can provide adequate protection during a temperature transient if coupled with a properly designed fuel block. When a coolant/fuel-block combination has a positive total coolant temperature coefficient, a coupled

neutronics/thermal-hydraulics assessment should be performed to determine the significance of the positive coefficient. It is also apparent that the lithium enrichment is significant for the LiF-BeF₂ coolant, but not for the LiF-NaF-ZrF₄ coolant; because the Zr constituent dominates neutron capture. Therefore, to achieve the optimum neutronic performance, the LiF-NaF-ZrF₄ coolant does not have to use extremely high ⁷Li enrichment (as is typically assumed).

4.3 SHORT-TERM ACTIVATION

The parasitic neutron captures in the salt activate the coolant materials, which results in the flow of additional, often radioactive, isotopes throughout the coolant circuit. Alpha and beta radiation cannot travel through the coolant pipes without being absorbed; therefore, the activation products of significant interest are high-energy gamma emitters. Many very short-lived activation products ($T_{1/2} < 1$ sec) are present but are insignificant because they will decay before traveling out of the reactor vessel. Many of these isotopes will be filtered out of the coolant during operation. The noble gases (helium, krypton, and most of the tritium) will come out naturally with no removal work required. The last traces of tritium can be gas-sparged under chemically reducing conditions. Carbon will not be in solution and can be removed. Therefore, these isotopes have been removed from our analysis of activation products. Figures 16 and 17 show the activation levels of the coolant options and their constituent components, respectively, at three time steps after the irradiation stops (either because the coolant left the core or because the reactor was shut down). The primary activation product in water is ¹⁶N ($T_{1/2} = 7$ s). Along with ¹⁶N, the two isotopes with similar half-lives and high-energy gamma emission that are significant in fluoride salts are ²⁰F ($T_{1/2} = 11$ sec) and ¹⁹O ($T_{1/2} = 27$ s). These two isotopes are the major contributors in the salt with the lowest activation level (LiF-BeF₂). Because there are no intermediate-lived activation products in this salt, after a single day, the activation levels are nearly zero, a level similar to water. However, because the 1-min activation levels are 5 orders of magnitude larger than water (on a per-unit-mass basis), online maintenance may be restricted.

Like sodium coolant, salts with a sodium component have a significant concentration of ²⁴Na ($T_{1/2} = 15$ h) when irradiated. This will impede refueling operations because the exposure levels will still be significant after a few days of decay. Potassium is naturally radioactive, due to ⁴⁰K, but with activation, a substantial amount of ⁴²K ($T_{1/2} = 12$ h) is produced (along with several other isotopes). This leads to very large activation levels for several days after irradiation ceases.

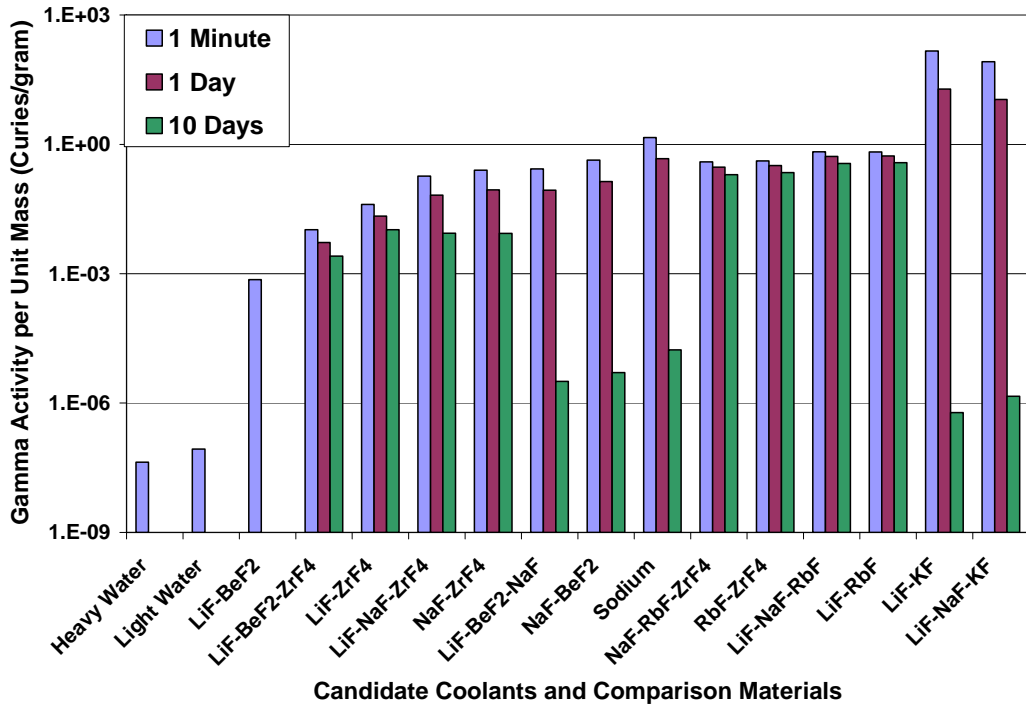


Fig. 16. Activity levels for candidate coolants and comparison materials.

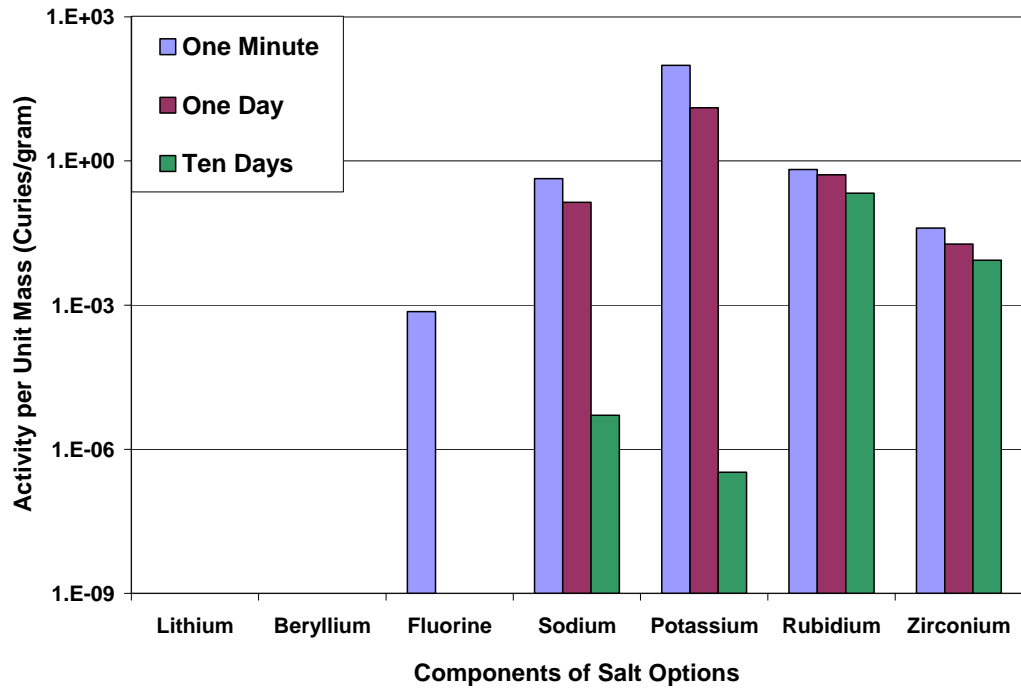


Fig. 17. Activity levels for components of various salt options.

Coolants with a rubidium component have several significant activation products (^{86m}Rb , ^{88}Rb , and ^{86}Rb) with a range of significant half-lives (1 min, 18 min, and 18 days, respectively) and high-energy (>0.3 MeV) gamma radiation. As shown in Figures 16 and 17, the activation level of rubidium salts due to ^{86}Rb is still significantly higher after 10 days than coolants without rubidium. Zirconium contains an even greater number of significant activation products (^{97m}Nb , ^{97}Nb , ^{97}Zr , ^{95}Nb , ^{95}Zr) with a range of half lives (1 min, 1 h, 17 h, 35 days, and 64 days), but the activity is less than that of rubidium by an order of magnitude for under 10 days of post-irradiation decay.

Based on activation factors, priority should be given to the LiF-BeF_2 salt; however, salts without a rubidium or zirconium component will decay to acceptable levels after several days, so that maintenance and refueling can be performed in close proximity to the coolant. For salts that contain zirconium or rubidium, the activated coolant could be pumped from the core and replaced with a clean salt for planned outages; or robotics could be used for refueling, maintenance, and inspection.

4.4 LONG-TERM ACTIVATION

Because of unstable isotopes produced by its prolonged irradiation, disposing of the coolant may present challenges at the end of the lifetime of the reactor. Therefore, we have also considered the transmutation of each coolant and the significant long-lived activation products produced. All types of radiation (alpha, beta, and gamma-ray emissions) were considered significant for long-term disposal.

Tables 16 and 17 show the activity levels of the coolant salts after 1 or 10 years of cooling following a 60-year exposure. To simplify the table, the activities are nominal values ($\pm 50\%$) for the indicated salt constituents irrespective of the specific coolant salt composition. For example, all candidate salts that contain beryllium were found to have a 1-year activity of $1.5\text{--}2.5 \times 10^{-7}$ Ci/g. As shown in Table 16, the activity of each coolant component is below 300 pCi per gram of coolant, and two orders of magnitude less for non-zirconium-containing salts. After 10 years of cooling (Table 17), these levels are reduced to the very long-lived isotopes, with ^{40}K (the naturally occurring isotope) being the only high-energy gamma emitter. The highest activity is from ^{36}Cl , produced by the (n,α) reaction with ^{39}K . Therefore, after a modest cooling period, the handling of all non-potassium salts should be relatively acceptable with minimal shielding. Sodium-22 has a very small activity (2 nCi/g) after 10 years and a comparably short half-life (3 years). Therefore, sodium, like lithium, does not pose a long-term risk for waste disposal.

Table 16. Nominal activity level of coolant constituents after 1 year of decay

Activated isotope	Radiation			Level of activation ($\mu\text{Ci/g-coolant}$) (parent elements in coolant)				
	Decay type	Gamma energy (MeV)	Half-life	Be	Na	K	Rb	Zr
^{10}Be	β^-		$1.5 \times 10^6 \text{ y}$	0.2				
^{22}Na	β^+, γ	1.3	3 y		0.02			
^{36}Cl	β^-		$3 \times 10^5 \text{ y}$			1		
^{40}K	β^-, γ	1.5	$1 \times 10^9 \text{ y}$			0.04		
^{84}Rb	β^-, γ		33 d				0.006	
^{86}Rb	β^-, γ		19 d				0.1	
^{87}Rb	β^-		$50 \times 10^9 \text{ y}$				0.02	
^{89}Sr	β^-, γ	0.91	51 d				0.02	
^{91}Y	β^-, γ		59 d					0.001
^{93}Zr	β^-, γ	0.03	$1.5 \times 10^6 \text{ y}$					0.4
^{95}Zr	β^-, γ	0.8	64 d					60
$^{93\text{m}}\text{Nb}$	β^-, γ	0.03	$1.5 \times 10^6 \text{ y}$					0.3
^{95}Nb	β^-, γ	0.8	64 d					100
$^{95\text{m}}\text{Nb}$	β^-, γ	0.2	64 d					0.7
<i>cumulative activity from coolant-constituent</i>				0.2	0.02	1.04	0.15	161
Total activity level ($\mu\text{Ci/g-coolant}$)								162

Table 17. Nominal activity level of coolant constituents after 10 years of decay

Activated isotope	Radiation			Level of activation ($\mu\text{Ci/g-coolant}$) (parent elements in coolant)				
	Decay type	Gamma energy (MeV)	Half-life	Be	Na	K	Rb	Zr
^{10}Be	β^-		$1.5 \times 10^6 \text{ y}$	0.2				
^{22}Na	β^+, γ	1.3	3 y		0.002			
^{36}Cl	β^-		$3 \times 10^5 \text{ y}$			1		
^{40}K	β^-, γ	1.5	$1 \times 10^9 \text{ y}$			0.04		
^{87}Rb	β^-		$50 \times 10^9 \text{ y}$				0.02	
^{93}Zr	β^-, γ	0.03	$1.5 \times 10^6 \text{ y}$					0.4
$^{93\text{m}}\text{Nb}$	β^-, γ	0.03	$1.5 \times 10^6 \text{ y}$					0.3
<i>cumulative activity from coolant-constituent</i>				0.2	0.002	1.04	0.02	0.7
Total activity level ($\mu\text{Ci/g-coolant}$)								2

Three of the isotopes listed in Table 17 (^{10}Be , ^{36}Cl , $^{93\text{m}}\text{Nb}$) are not specifically addressed in the 10 CFR 61 regulations for control of low-level waste [41]. Chlorine-36 occurs in relatively high concentrations in potassium salts and has a high ingestion dose conversion factor and a high environmental mobility. Therefore, it poses a potential risk for long-term migration from a low-level waste (LLW) disposal facility, especially in a contaminated well/drinking water exposure scenario, which must be analyzed for the licensing of a LLW facility. However, ^{36}Cl can be easily separated from the salt and disposed of separately. Beryllium-10 is a long-lived beta emitter with unknown environmental mobility properties. The parent to $^{93\text{m}}\text{Nb}$ is ^{93}Zr , which is very long-lived (1.5 million years) and cannot be easily removed from the constituent salt. Although $^{93\text{m}}\text{Nb}$ poses the greatest long-term disposal risk of the salts considered, its activity level after 60 years of use in an AHTR appears to be sufficiently low to qualify as LLW.

5. COST OF THE SALT

There are many important economic factors to be considered with respect to selecting coolant; however, at this stage of the AHTR design, it is most useful to focus on the cost of acquiring the salt coolant. The most important “salt cost” is that associated with a significant deployment of the AHTR. Unfortunately, we cannot predict this cost because many of the constituents of candidate salts are not commodity chemicals, and the cost associated with deploying significant numbers of AHTRs would swamp the existing markets and change the price that is offered.

However, there are some basic trends and facts that can be used to help understand the classification and costs of various salt constituents. In 1971, ORNL conducted a survey of potential coolants that could be used as the secondary coolant in the MSBR design [5]. In the context of this survey, solicitations were made to vendors to provide prices for candidate salts. The goal was to establish an estimate of the unit prices required for supplying the coolant inventory (~280,000 liters) for a 1000-MWe MSBR plant. Some vendors could not supply estimates for an order this large, and extrapolation methods were employed to refine the estimates when possible. The results of these 1971 price estimates are shown in Table 18. A more recent survey of commodity [42] pricing for relevant salt constituents is included as Table 19.

Based on the 1971 study and the more recent commodity values, it is evident that the constituents of candidate coolants fall into three categories: (a) relatively inexpensive commodity chemicals (NaF); (b) moderately expensive specialty materials produced on a large scale (Zr-

Table 18. Price estimate of salt coolants in 1971 (U.S. dollars)

Coolant	Composition (%)	Melting point (°C)	Cost (\$/kg)	Cost (\$/liter)	
<i>AHTR candidate coolant salts</i>					
NaF-KF-ZrF ₄	mol %	10-48-42	385	4.6	11.7
	wt %	4-27-69			
⁷ LiF-NaF-KF	mol %	46-11.5-42.5	454	11.3	24.1
	wt %	29-12-59			
⁷ LiF-NaF-BeF ₂	mol %	35-27-38	335	17.5	35.0
	wt %	24-46-30			
⁷ LiF-BeF ₂	mol %	67-33	460	26.3	52.2
	wt %	53-47			
<i>Other industrial salts</i>					
NaNO ₃ -NaNO ₂ -KNO ₃	mol %	7-48-45	142	0.33	0.57
NaF-NaBF ₄	mol %	8-92	385	0.82	1.5
LiCl-KCl	mol %	59-41	355	1.12	1.8
<i>Other low-vapor pressure coolants</i>					
Pb			327	0.4	4.1
Na			98	0.88	0.72
Pb-Bi			125	7.45	74.4
Bi			271	13.2	129

Table 19. Commodity Prices for Selected Materials

Material	Commodity price ^a (\$/kg)	Price of contained metal \$/kg-metal	Derived fluoride price (\$/kg-fluoride)	World-wide production (ton/y)
LiF	17.00	63.54	63.54	--
Li ₂ CO ₃	1.72	9.16	2.45	~50,000
BeO	100.00	610.00	117.00	--
Be-metal	770.00	770.00	147.4	--
11% BeO-ore	0.080	2.02	--	114 (Be element)
Zr-metal	30.80	30.80	16.80	--
ZrO ₂	8.89	11.89	6.48	--
98% ZrO ₂ -ore Baddeleyite	3.00	4.05	2.2	21,300
NaF	1.37 ^b	2.56	1.32	very large

^aAll prices are from the USGS Minerals Yearbook except NaF. USGS prices are for 2002 except LiF (1995) and Li₂CO₃ (2004).

^bPrice from *Chemical Marketing Reporter* volume 267(12) p.18.

metal, LiF); and (c) very expensive specialty materials (^7LiF , Be). For the 1971 study, the price of 99.995% ^7Li was assumed to be \$120/kg-LiF. Some of the values for Zr-prices in Tables 18 and 19 do not reflect the cost associated with hafnium removal.

It is possible that this classification could change for some constituents based on market factors not yet considered. For example, there are two alternative raw material sources for obtaining hafnium-free ZrF_4 : (a) recovery of irradiated cladding and fuel-element hardware, and (b) recovery of ZrF_4 from spent pickling-solution streams (from hafnium cleaning of Zircalloy). It is also possible that the market could change the specialty prices associated with RbF and KF compounds. Alkali ores possess considerable amounts of Rb and K minerals that remain unused and accumulate in tailing piles. Rubidium has an unusual position with respect to markets. While the world market for rubidium is extremely small (4 tons/year), it ranks as the 23rd most abundant element on earth (16th most abundant metal)—more abundant than copper, lead, and zinc; and much more abundant than lithium or cesium.

6. CHEMICAL CONSIDERATIONS

6.1 BACKGROUND, CONTEXT, AND PURPOSE

The purpose of this section is to provide an assessment of key chemical factors related to the choice of the primary coolant for the AHTR. The most important chemical factor in this selection concerns the maintenance of acceptably small levels of corrosion for the metal alloy that will serve as primary containment. Alloy corrosion is the key materials-compatibility issue that is influenced by salt chemistry. Section 2 contains a review of candidate AHTR coolants and their properties, and Table 2 lists potential candidate salts. The review of coolant properties represents an update, a correction, and an extension of the previous summaries conducted many decades ago [10, 43].

The application of molten salt coolants is based on a 50-year history of molten salt nuclear technology, principally at ORNL. To appreciate the merits of using such high-temperature liquids as coolants in AHTRs, it is worthwhile to review some of that history as it pertains to AHTR applications. Although many more-extensive reviews of molten salt reactors exist, these might be too expansive in scope for those interested only in specific topics such as those concerning AHTR technology. Therefore, this overview will focus on key aspects in the development of these unique high-temperature fluids as they pertain to AHTRs. This report will

then focus in detail on these key elements that will lead to consideration of molten salt coolants for further development.

The use of molten salts in nuclear reactors has been an evolutionary process that included the parallel development of containment materials, physics, engineering, etc. Necessarily, this broad effort required the commitment of a large number of scientists and engineers over at least three decades. It is worth emphasizing that the use of molten salts was not originally envisioned but instead appeared as part of the evolutionary process to meet design requirements.

6.1.1 Aircraft Nuclear Propulsion (ANP) Project

In the 1950s, a nuclear-powered strategic bomber was conceived that could stay aloft for more than a month and be diverted to a target should the necessity arise in this era of the Cold War. To power such an aircraft, a test reactor—the Aircraft Reactor Experiment (ARE)—was constructed [44]. A major requirement for this reactor was that it have a very high power density to keep the weight in the aircraft at a minimum. Originally, a more conventional design of solid fuel pins with liquid metal (sodium) was planned. However, the need for the high power density and safety could not be met with solid fuel, which might be inadequately cooled in such a design.

Therefore, it was decided to develop a liquid fuel that could operate at a high power density and that was inherently safe because of a negative power coefficient. In other words, if the reactor power went up excessively, the thermal expansion of the fluid fuel would cause a natural lowering of the amount of fuel in the core and thus decrease the overall reactor power. A search then began for a high-temperature fluid that would satisfy the following requirements [4]:

1. Consist of elements of low-neutron-capture cross-section.
2. Dissolve more than the critical concentration of fissionable material at temperatures safely below the temperature at which the fuel leaves the heat exchanger.
3. Be thermally stable with low vapor pressure over the operating temperature range.
4. Possess heat transfer and hydrodynamic properties adequate for its service as a heat-exchange fluid.
5. Be relatively nonaggressive toward some otherwise suitable material of construction, presumably a metal, and toward some moderator material.
6. Be stable toward reactor radiation and be able to survive fission of the uranium or other fissionable material. Must tolerate fission-product accumulation without serious deterioration of its useful properties.
7. Be relatively inexpensive and capable of an economical reprocessing scheme.

Various inorganic compounds such as halides, nitrates, hydroxides, and carbonates were considered, and many of these were tested in the laboratory, primarily for corrosive action on potential container materials. Of these many classes of inorganic compounds, fluorides were deemed much more suitable for reasons that include improved neutron economy, better moderating efficiency, higher chemical stability, lower vapor pressure, higher specific heat, and usefulness of the element without isotope separation [45].

For the ARE, a mixture of NaF and ZrF₄ was used as the fluoride solvent [46] for the UF₄ fuel component to make a solution of NaF-ZrF₄-UF₄ (53.09-40.73-6.18 mol %). The containment metal used for this liquid fuel mixture was a nickel-base alloy, Inconel, (15% Cr, 7% Fe, balance Ni.) [47]. Although it was initially planned to use a sodium-cooled, solid-fuel-element reactor, the reactor design evolved first to that of a sodium-cooled, stationary-liquid-fuel reactor and finally to that of a circulating-fuel reactor employing sodium as a coolant for the reflector [46]. The ARE operated in November 1954 for 221 h at a maximum thermal power of 2.5 MW.

Postoperative examination of the reactor components [48] plus experimental corrosion-loop testing revealed that Inconel corrosion was excessive for long-term operation but could be improved by adding molybdenum to the alloy. Furthermore, corrosion loops indicated that Inconel was more severely corroded with fuel salts made with all alkali-metal fluorides than those made with NaF-ZrF₄ mixtures, suggesting that the chemical composition of the fuel salt played a significant role in controlling the corrosion chemistry. Extensive development in materials research [49–53] resulted in the production of an improved nickel-base alloy, INOR-8 (17% Mo, 7% Cr, 5% Fe, balance Ni).

The period following the successful operation of the ARE evolved to the design and prototype construction of an Aircraft Reactor Test (ART). The work progressed with further development and testing until the Atomic Energy Commission terminated the ANP project in 1957 [54]. This novel molten salt technology was then turned to civilian interests in the development of molten salt breeder reactors with the design and construction of the MSRE.

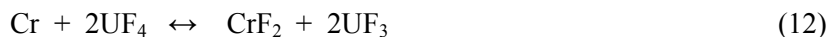
6.1.2 Molten Salt Reactor Experiment

The MSRE represented the first step in developing a breeder reactor. To this end, it was necessary that the molten solvent components consist of elements with especially low thermal neutron cross-sections in order to achieve the highest possible breeding ratio in the breeder reactor prototype [55]. The MSRE was planned to test the combination of new components and the overall reactor design—without including the breeding stage.

It was constructed of INOR-8 (now identified as Hastelloy N) for improved corrosion resistance and fueled with LiF-BeF₂-ZrF₄-UF₄ (64-30-5-1 mol %). The LiF component was

enriched Li-7 for better neutron economy. Neutron moderator graphite filled the reactor core in the shape of rectangular stringers that provided channels for the circulating fuel. The fuel was circulated from the reactor core at 650°C to a heat exchanger operating at 550°C.

Corrosion in the reactor circuit was controlled by reducing approximately 1% of the UF₄ solute to UF₃, so that the oxidative equilibrium between the chromium of the Hastelloy N container was shifted to the left:



Postoperative examination of the reactor container showed that corrosion was successfully minimized by this redox method of control. It was observed that the fuel salt produced only very minor, barely detectable levels of corrosion, whereas for the coolant salt, the corrosion was not detected at all [56].

Further postoperative examination showed that fission-product tellurium diffused into the Hastelloy N grain boundaries and caused an unacceptable stress-cracking embrittlement of the metal. Radiation hardening of the Hastelloy N and diffusion of tritium (produced by the action of the neutrons on the lithium component of the solvent) were also of concern for future reactor applications.

6.1.3 Molten Salt Breeder Reactor

In 1972, following the success of the MSRE operations and encouraging R&D solutions to the postoperative findings, the next step in development was to move toward a breeder reactor [57]. However, competition with the broad Liquid Metal Fast Breeder Reactor (LMFBR) program curtailed further extensive progress. Nevertheless, significant developments in two areas of interest are worthy of recognition: materials and fuel salt chemistry.

This historical overview covering the development of molten salt technology over several decades should demonstrate how various aspects evolved. The selection of an appropriate molten salt medium and the effects on the container material (corrosion) are the two subjects of focus in this report. They will be discussed separately with recommendations, as appropriate, for application to coolant technology.

6.2 MATERIALS FOR HIGH-TEMPERATURE FLUIDS

Inconel was originally found to be superior to non-nickel-base alloys and therefore used in the ARE. However, the extent of corrosion was still excessive for prolonged reactor operations. As a result, an alloy development program was initiated based on the encouraging results found

with Inconel [52]. Studies were started [63] on the Ni-Mo system, which exhibited excellent corrosion properties both from the standpoint of measurements of equilibrium solubilities on various metals in salt mixtures and on the basis of tests that were made with the commercial alloy Hastelloy B (composition: 29% Mo, 5% Fe, balance Ni). Corrosion rates for this alloy were found to be quite low at temperatures in excess of 900°C and very much lower than those for Inconel under comparable conditions. However, Hastelloy B suffered from several adverse characteristics. Poor fabricability and embrittlement after operation between 650°C and 815°C, coupled with poor oxidation resistance at elevated temperatures, disqualified Hastelloy B despite its excellent corrosion resistance.

In developing an improved nickel-base alloy containing chromium for long-term salt service it was found that a significant change in the oxidation rate* occurs at about 6% Cr. At this composition, the oxide changes from the NiMoO₄ type to one that is predominantly the Cr₂O₃ type [58]. Since a high chromium content is undesirable from the standpoint of fused fluoride corrosion, only a slight excess of chromium is desired for the proposed alloy. Molybdenum, which strengthens nickel alloys, was reduced in amount to the point that a solid solution of nickel and molybdenum would be stable at all temperatures of interest.

On the basis of extensive testing, an alloy designated as INOR-8 (now identified as Hastelloy N with composition 17% Mo, 7% Cr, and 5% Fe, balance Ni) was selected as the most promising container material for fused fluorides. Interestingly, the iron content was included so that the chromium could be added as ferrochromium rather than pure chromium with the resulting decrease in costs. This alloy served the operation of the MSRE in an excellent fashion, and it was only after reactor operations that some deficiencies were observed.

As stated in Sect. 6.1.2, postoperative examination of the MSRE revealed the damaging effects of fission-product tellurium, resulting in the development and testing of modified alloys for future containment purposes. It was found that additions of titanium or niobium produced a modified Hastelloy N alloy that had good resistance to both radiation embrittlement and intergranular cracking by tellurium [59,60]. Furthermore, it was seen that controlling the molten salt oxidation potential had dramatic effects on the extent of cracking [61] as shown in Figure 18. This technique of salt chemistry control by redox changes was performed during the operation of the MSRE and known even before then as a technique for preventing corrosion of all metal alloys, is clearly one of the best means of corrosion control. Consideration of redox control is an integral and important factor for salt selection for AHTR service and for the system design.

* "Oxidation" as opposed to "corrosion," realizing that the other side of the container is exposed to the atmospheric environment.

EXTENT OF TELLURIUM EMBRITTLEMENT OF HASTELLOY N
IS STRONGLY AFFECTED BY OXIDATION POTENTIAL OF SALT.

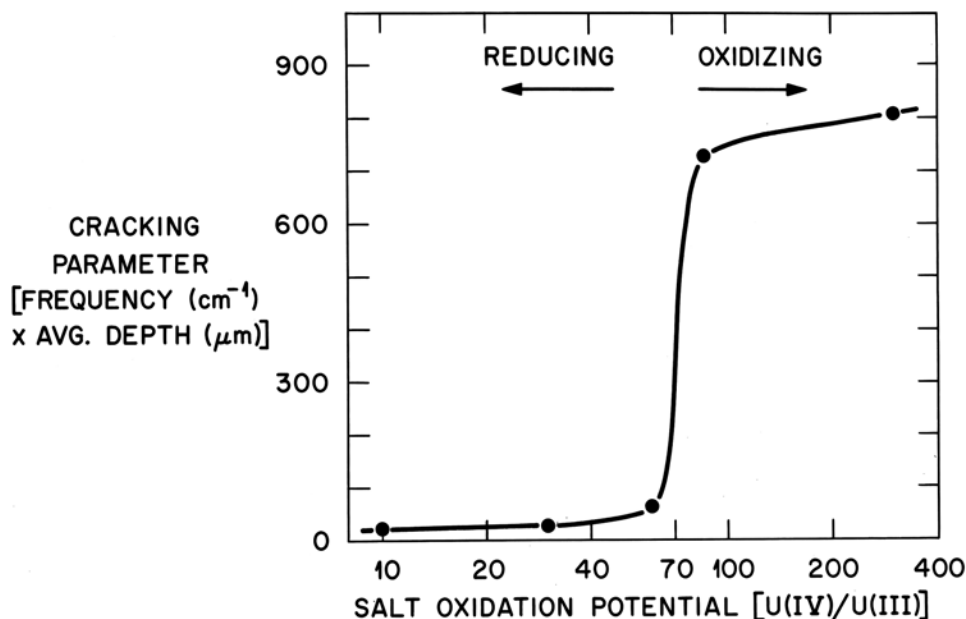


Fig. 18. Effect of redox potential on tellurium cracking of Hastelloy N.

6.3 CHEMISTRY OF MOLTEN FLUORIDE SALT COOLANTS

The selection and effective use of molten salts as high-temperature coolants depends on an understanding of the chemistry. Of major importance in this understanding are:

(1) the ability to produce and maintain a high level of purity, (2) phase diagram behavior for mixtures, (3) the utilization of acid-base effects, and (4) the control of the redox potential of the salt medium as it affects corrosion and other chemical processes.

6.3.1 Salt Purification

Molten salt use typically begins with the acquisition of raw components that are combined to produce a mixture that has the desired properties when melted. However, most suppliers of halide salts do not provide materials that can be used directly. The major impurities that must be removed are moisture/oxide contaminants, to prevent severe corrosion of the container metal. Once removed, these salts must be kept from atmospheric contamination by handling and storage

in sealed containers. During the ANP/MSRE era, a considerable effort was devoted to salt purification by HF/H₂ sparging of the molten salt and is described in numerous reports [45, 52, 62–64]. Besides removing moisture/oxide impurities, the purification also removes other halide contaminants, such as chloride and sulfur. The sulfur is usually present in the form of sulfate and is reduced to sulfide ion, which is swept out as H₂S in the sparging operation. Methods were also developed to ensure the purity of the reagents used to purify the salts and to clean the container surfaces used for corrosion testing.

Another means of purification that can be performed after sparging involves simply reducing the salt with a constituent active metal such as an alkali metal, beryllium, or zirconium. While such active metals will remove oxidizing impurities such as HF, moisture, or hydroxide, they will not affect the other halide contaminants that affect sulfur removal. Therefore, it seems inevitable that the HF/H₂ sparging operation, either by itself or followed by a reducing (active metal) treatment, will be a necessity.

Although a great deal of effort can be devoted to purifying the molten salt mixture in the manner described above, it is primarily useful in producing materials for research purposes without the possibility of interference from extraneous impurities. In the final application of molten salts, one can envision that a less strenuous and less expensive purification treatment might suffice for high-temperature-coolant purposes.

6.3.2 Phase-Diagram Behavior

Salt components by themselves often have melting points and/or other properties that preclude their use. For example, the alkali fluorides individually have melting points in excess of 800°C, which make them difficult to use alone as a liquid medium. However, the combination of two or more of these component salts can produce low-melting mixtures that satisfy the melting point requirements of a system. Furthermore, some properties of individual components, such as viscosity (for pure BeF₂) or vapor pressure (for pure ZrF₄), are reduced along with the resulting melting point by combination with other salt components. For these reasons, a large effort had been devoted to the study of phase diagrams for various mixtures of fluoride salts.

While many combinations are documented in various references [6–7] it is conceivable that the phase diagram of some salt mixture for high-temperature-coolant applications has not been determined. Particular salt systems are discussed in Sect. 2.

6.3.3 Acid-Base Chemistry

A less obvious but equally important chemical aspect is that of the molten-salt acid-base chemistry. To put it in proper perspective, one should realize that an aqueous chemical process

could never be developed without controlling of the acid-base properties of the solution, because most chemical processes simply do not work well otherwise. Similarly, this control can be essential in molten salt chemistry. The major obstacle in understanding the acidity effect is in comprehending the nature of this Lewis acid-base property, in which an acid is defined as an electron pair acceptor and a base as an electron pair donor. For molten fluorides, ZrF_4 , UF_4 , and BeF_2 would be examples of Lewis acids. These acids would interact with a Lewis base, F^- , in the following fashion:



Salts that easily give up their fluoride ions—the alkali metal fluorides—interact with the acidic salts that accept them to form complexes as shown in Eq.13. The effect of such complexation is a stabilization of the acidic component and a decrease in the chemical (thermodynamic) activity. Although these concepts were realized in the early developmental stages of molten salt chemistry, a more macroscopic (thermodynamic) view of solvent changes was taken and resulted in the laborious measurement of activity coefficients for individual components in specific salt mixtures. A classic presentation [65] of activity coefficients for numerous fluoride salts (Fig. 19) as a function of increasing LiF content (i.e., increasing basicity) in the LiF- BeF_2 mixtures formed the basis for much of the understanding of that time. It was invaluable for predictions of equilibrium concentrations of reactive components in these solutions. Prior to that, there were such suggestive observations [55] that corrosion of Inconel was much worse with the ternary alkali metal fluoride eutectic (a basic salt solution) than with NaF- ZrF_4 (an acidic salt solution) containing UF_4 . We now explain this as being due to an increase in the stability of the corrosion product by complexation with the higher activity of the fluoride ions in the basic salt mixture. Such acid-base properties are also seen in the viscosity decrease of acidic BeF_2 (viscous because of cross-linking through a Be-F-Be bridging network) with additions of the basic component F^- to form monomeric BeF_4^- ions of normal solution viscosity (~1–10 cP):



Acid-base effects are also seen in vapor-pressure changes of volatile ZrF_4 to form the nonvolatile ZrF_6^- ion:



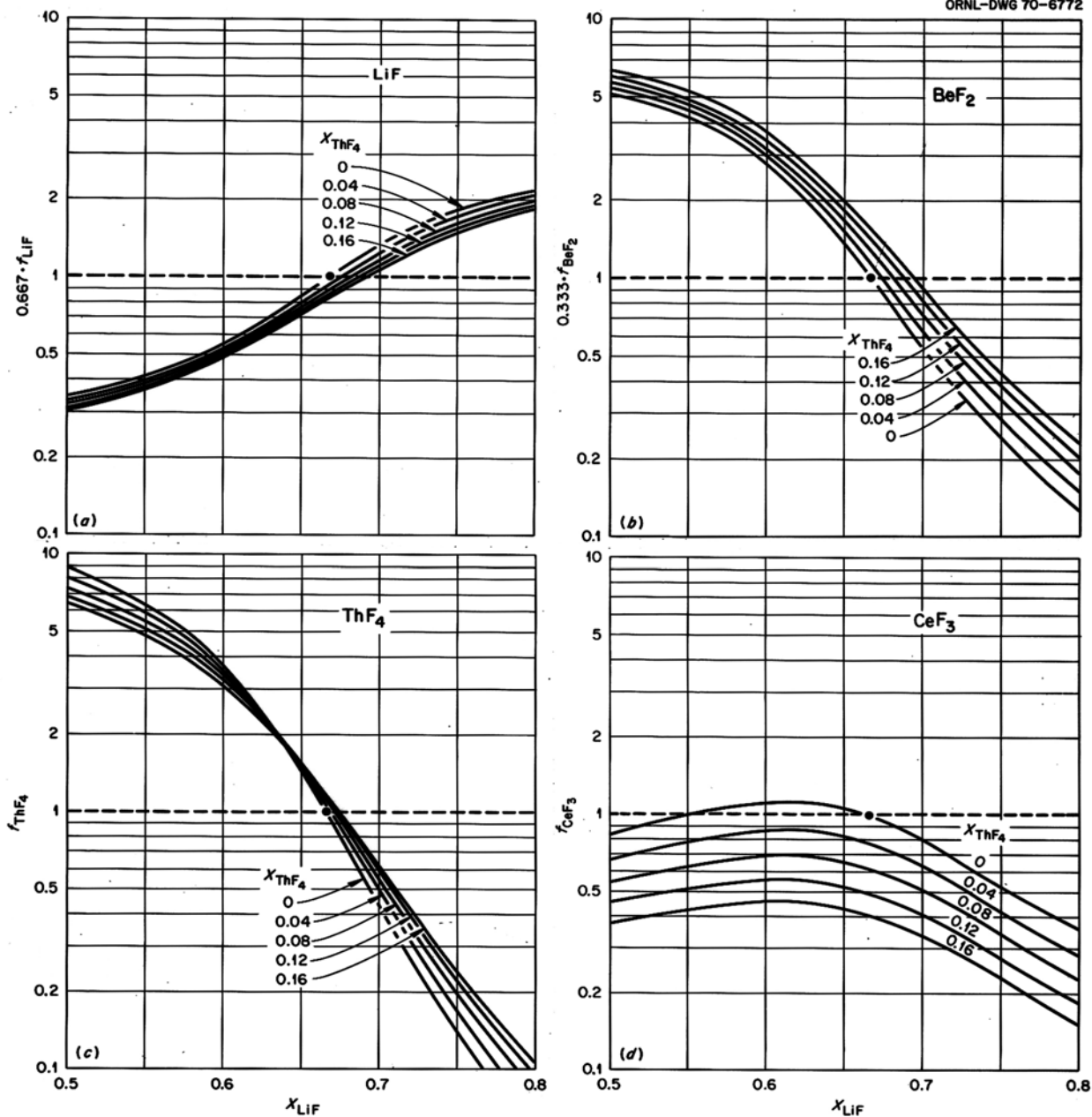


Fig. 19. Activity coefficients of various components versus LiF content, showing acid-base effects on metal ions in solution. (Standard state is $2LiF \cdot BeF_2$.)

Today, the understanding of the more microscopic coordination chemistry of these systems through the use of various spectroscopies that can identify the coordination behavior of the ions enables a prediction of these chemical equilibrium shifts, at least on a qualitative scale. Acid-base chemistry then becomes an essential factor in the selection of constituents for high-temperature coolants.

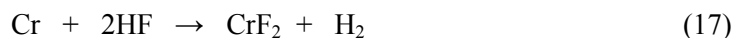
6.3.4 Corrosion Chemistry

Corrosion has long been a major problem in the use of metals and is a major concern in using such materials for containment purposes. Consequently, years of study have been devoted to corrosion chemistry in various media, but especially in aqueous solutions. Indeed, this same concern has prevailed for metallic containment of molten salts and was actively pursued throughout the years of development.

Unlike the more conventional oxidizing media, the products of oxidation of metals by fluoride melts tend to be completely soluble in the corroding media [58]; hence, passivation is precluded and corrosion depends directly on the thermodynamic driving force of the corrosion reactions [50]. Design of a chemically stable system utilizing molten fluoride salts, therefore, demands the selection of salt constituents that are not appreciably reduced by available structural metals and the development of containers whose components are in near thermodynamic equilibrium with the salt medium.

Examination of the free energies of formation for the various alloy components in Inconel or Hastelloy N shows that chromium is the most active of the metal components. Therefore, any oxidative attachment to these nickel-base alloys should be expected to show selective attack on the chromium. Such oxidation and selective attack follow from reactions such as the following (in Eqs. 16–19) [4] for the fuel salt:

Impurities in the melt with dissolution of the CrF_2



Oxide films on the metal



These reactions are followed by reaction of NiF₂ with Cr:

Reduction of UF₄ to UF₃



Of course, in the case of a coolant salt with no fuel component, reaction (19) would not be a factor.

Redox processes responsible for attack by molten fluoride mixtures on these alloys result in selective oxidation of the contained chromium. This removal of chromium from the alloy occurs primarily in regions of highest temperature and results in the formation of discrete voids in the alloy [66]. These voids are not, in general, confined to the grain boundaries in the metal but are relatively uniformly distributed throughout the alloy surface in contact with the melt. The rate of corrosion has been measured and was found to be controlled by the rate at which chromium diffuses to the surfaces undergoing attack [52].

6.4 COOLANT SALT SELECTION FACTORS RELATED TO CORROSION

From the list of potential coolant salts, none are intrinsically corrosive to the metal alloy components. This view is based on the thermodynamic stability of the fluoride components relative to those of the alloy metal and is described in depth by Grimes [4] and summarized here in Sect. 6.3.4, Corrosion Chemistry. Furthermore, it has been demonstrated over the past several decades in systems operating up to 850°C.

Nevertheless, the evidence for selecting a coolant based on corrosion is not adequate at present. Previous studies focused on the corrosion by salts containing uranium, in which uranium is the key factor in the intensity and nature of alloy corrosion [cf., Eq. (19)]. A good understanding of fuel-salt corrosion was developed, but we do not know the precise mechanism of persistent (i.e., mass-transfer) corrosion of nickel alloys with coolant salts. We must assume that redox-sensitive species, such as Cr(II/III) and Fe(II/III), are important factors in this process [51, 67]. However, with limited analytical resources, other factors apparently present in previous studies must be evaluated to identify all truly significant trends.

6.4.1 Oxidation State of Corrosion Products [68]

During the ANP program, a continuing effort was made to understand the oxidation state of corrosion products such as Cr, Fe, and Ni in different salts. Although these studies were crude by today's standards, the basic trends of oxidation state stability, shown in Table 20, were apparent and helped explain the corrosion phenomena that were being observed in fuel salts.

Table 20. Predominant oxidation states of dissolved alloy constituents in various molten salts

FLiNaK	Cr(III)	Fe(II/III)	Ni(II)
NaF/ZrF ₄	Cr(II)	Fe(II)	Ni(II)
2LiF/BeF ₂	Cr(II)	Fe(II)	Ni(II)

It is apparent that FLiNaK has a distinct behavior. As a strongly basic solvent, it would tend to stabilize the M(III) oxidation state and could provide for a stronger corrosion driving force due to the variation between cation [Cr(II/III), Fe(II/III)] oxidation states with temperature.

6.4.2 Temperature Dependence of Dissolved Chromium Concentration [69–71]

The equilibrium level of dissolved chromium has been measured for fuel salts, but not for coolant salts. Although the information on fuel salts is not directly applicable to coolants, we expect that fuel systems that experience minimal corrosion would also be better coolants. Review of the dissolved chromium levels for various fuel salts in Table 21 again reveals that FLiNaK stands somewhat apart from the other salts as supporting a higher degree of corrosion. It also appears that there is some benefit in avoiding a very acid (high-ZrF₄ or BeF₂-content) system and that a salt mixture that has a nearly complete coordination shell (2:1 ratio of alkali halide to Zr or Be and heavier alkali salt) has the least potential for supporting corrosion based on the temperature sensitivities shown in Table 21.

This approach is a significant oversimplification, as the identity of the various species is very important. For example, the saturating species that contain chromium is different for each of these salts. However, for a first approximation, Table 21 provides a useful guide.

6.4.3 Polythermal Corrosion Test Loops with Coolant Salts

Although less than 10% of all corrosion testing was done with salts that were free of uranium, this small fraction amounts to a significant body of work because of the extensive test program that was carried out. The results of testing for uranium-free salts are summarized in Table A.1 in the appendix.

Table 21. Equilibrium level of dissolved metals for pure elements in contact with various fuel salts

Salt mixture	Mol % ZrF ₄ or BeF ₂	[UF ₄] mol %	[Cr] at 600°C ppm	[Cr] at 800°C ppm
FLiNaK	0	2.5	1100	2700
LiF-ZrF ₄	48	4.0	2900	3900
NaF-ZrF ₄	50	4.1	2300	2550
NaF-ZrF ₄	47	4.0	1700	2100
NaF-ZrF ₄	41	3.7	975	1050
KF-ZrF ₄	48	3.9	1080	1160
NaF-LiF-ZrF ₄ (22-55-23)	23	2.5	550	750
LiF-BeF ₂	48	1.5	1470	2260

A quick inspection of this table reveals that Hastelloy N (INOR-8), just as it is for fuel salts, is a superior choice (rather than Inconel or SS) for coolant salts. The corrosion is so intense and the duration so short for most Inconel loops that it is hard to make a judgment about which salt supports the least corrosion. It is clear that FLiNaK is certainly among the worst. For INOR-8 loops, the corrosion is so minor that it is hard to sort out corrosion effects due to the salt's composition. Some additional Inconel loop tests [72–73] were conducted with special fuel salt mixtures in which the ZrF₄ and BeF₂ concentrations were varied in an attempt to select the best composition. However, these tests were somewhat inconclusive because of the short test duration (500 h) and the impurity effects. Within the resolution of these tests, the trends indicated in Table 21 were verified: very basic (FLiNaK) and very acidic (LiF-ZrF₄) salts showed the worst performance. *Nevertheless, the proper control of redox factors, as described in Sect 6.4.4, can make even these salt mixtures acceptable with respect to corrosion.*

6.4.4 Redox Control Factors

At various periods at ORNL, the control of the oxidation-reduction state of the salt was explored as a means to minimize corrosion. During the ANP period, this approach was found to be somewhat effective. However, it was not practical, because strong reductants either reduced zirconium or uranium in the salt to a metal that plated on the alloy wall or resulted in some other undesirable phase segregation. During the MSRE operation, periodic adjustment of the U(III)/U(IV) ratio was effective in limiting the corrosion in the fuel circuit. Keiser also explored the possibility of using metallic beryllium to reduce corrosion in stainless steel containing a LiF-BeF₂ salt [74]. This treatment was effective only as long as the solid beryllium was immersed in the salt. There was little, if any, buffering capacity in this salt to maintain the

reducing environment throughout the melt. Del Cul et al. have identified and tested candidate agents that could be used as redox buffers to maintain a reducing environment in the coolant circuit [75].

None of these redox-control strategies have been developed to the extent that we can rely on them for a definite salt selection. However, we can make some useful observations in this regard. For a lower-temperature system ($<750^{\circ}\text{C}$), it appears that Hastelloy N is fully capable of serving as a containment alloy without the need for a sophisticated redox strategy. Even an alkali fluoride such as FLiNaK could be suitable.

For temperatures in excess of 750°C and for alloys that will contain more chromium (as most higher-temperature alloys do), it appears that a reducing salt will be needed to minimize corrosion. Inconel without the benefit of a reducing environment was found to be unsuitable for long-term use. Only a mildly reducing environment is possible with a ZrF_4 -containing salt since a strongly reducing redox potential would reduce ZrF_4 , itself. Much more reducing systems can be devised with either FLiNaK or BeF_2 salts. Some very important material compatibility issues will have to be explored in order to use a highly reducing salt at these higher temperatures, because events such as carbide formation and carburization/ decarburization of the alloy (not discussed in the report) become a significant threat.

Should low-chromium/chromium-free alloys or suitable clad systems be devised as a container, then these problems with salt selection will largely disappear. However, in the absence of this solution, it appears that there are two strategies: (1) select a salt that should support the minimum level of corrosion in the absence of a highly reducing environment (some ZrF_4 salts, BeF_2 salts) or (2) select a salt with a large redox window that can be maintained in a highly reducing state (FLiNaK, BeF_2 salts). Given the expense and difficulty of doing development work with beryllium-containing salts, it seems logical to explore the most promising ZrF_4 salts without strong reductants and to explore FLiNaK with strong reductants and/or redox buffers.

7. CONCLUSIONS AND RECOMMENDATIONS

7.1 CONCLUSIONS

Based on the preceding review of nuclear, physical, chemical, and economic properties of candidate salts for the AHTR, the following conclusions were reached:

Salts composed of low-atomic-weight constituents (“light” salts) possess superior heat-transfer metrics for use as the AHTR coolant. Heavier salts are also relatively good coolants and would likely prove acceptable for design purposes.

Analysis indicates that the key reactivity coefficients (and their net effect) that control response to transients are more strongly affected by parameters associated with the fuel-block design (coolant volume fraction, poison level, and distribution) than by the identity of the particular salts under consideration. A computational framework was developed to evaluate these factors and was used to evaluate the various candidate salts. It appears that acceptable fuel-element designs can be found for most of the salts used in this study.

Activation levels in AHTR candidate coolants appear to be acceptable from both an operational and long-term disposal standpoint. Only the LiF-BeF₂ salts are very low-activation materials that support minimal shielding requirements. The other salt coolants have operational characteristics similar to those of sodium-cooled reactors. The disposal of all of the salt candidates as LLW after 60 years of operation and 10 years of cooling should be possible, although some simple pre-treatment may be required for certain coolants.

No consensus exists to select a particular salt based on its corrosion behavior with high-temperature alloys.

A number of the ZrF₄-containing salts appear to offer the best potential for achieving a low-cost coolant. The economic basis for these judgments is very important for the selection of a candidate and needs to be refined.

7.2 RECOMMENDATIONS

The selection of a suitable coolant salt should be based on numerous factors, including chemical, physical, nuclear, metallurgical, and economic factors. It is evident from past decades of experience that fluoride melts have an established advantage over the few other coolants that had been considered previously for extreme-temperature service (>700°C). The following remarks are directed primarily toward selection based on chemical factors that relate to corrosion, with the understanding that the overall assessment will need to account for other factors.

Proper selection of a coolant salt based on chemical differences is based largely on the acid-base properties of the combination, as described in Sect. 6. Both predictions and measurement of the container-metal-fluoride equilibrium concentrations are higher in basic salts as compared with neutral or acidic media. Some corrosion loop experience tends to corroborate this observation. Unfortunately, however, no systematic study of such a phenomenon has been made during these experiments.

A neutral or slightly acidic salt melt would be predicted to be the most advantageous with respect to corrosion behavior. However, basic salt melts tend to have significantly lower vapor pressures and lower viscosities, and these properties might present a problem (for example, ZrF₄

and BeF₂). Therefore, any selection of a coolant based on chemical considerations must, necessarily, be a compromise of all factors that might affect performance.

In this regard, it is recommended that two types of salts should be studied in the future:

- (1) Salts that have been shown in the past to support the least corrosion and are neither strong Lewis acids nor strong Lewis bases (i.e., “neutral”). Salts containing BeF₂ and ZrF₄ in the concentration range 25–40 mol % fall into this category.
- (2) Salts that provide the opportunity for controlling corrosion by establishing a very reducing salt environment. The alkali-fluoride (FLiNaK, FLiNaRb) salts and the BeF₂-containing salts fall into this category.

It is too early to make final recommendations for exact salt compositions, since the particular salt composition to be chosen will need to be determined from a carefully conducted trade study that balances the various selection factors for a particular reactor design.

7.3 CANDIDATE SALTS

Separate recommendations are made for work in the future with respect to (a) analysis and computations, and (b) experimental work. These recommendations do not constitute a final selection, rather they identify important candidate salts that exhibit important properties that should establish useful boundaries for future evaluations.

Further computational analysis of AHTR candidate salts is recommended on the following basis:

1. ZrF₄-salts that have the potential for low cost and special properties:
 - NaF-ZrF₄ and related ternary mixtures :
 - i. NaF-ZrF₄ (59.5-40.5) *potentially least expensive*
 - ii. ⁷LiF-NaF-ZrF₄ (42-29-29) *very low vapor pressure*
 - iii. RbF-NaF-ZrF₄ (34.5-24-41.5) *low melting point (420°C)*
2. BeF₂-salts that have superior nuclear properties and heat-transfer performance:
 - NaF-BeF₂ *low melting point salt (340°C)*
 - ⁷LiF-BeF₂ *neutron transparent salt, very low activation*

All alkali fluoride compositions require significant amounts of ⁷Li, and the mixtures with the most favorable heat-transfer properties (FLiNaK) have the poorest neutronic performance. The BeF₂ and ZrF₄ salt systems both have compositions that melt below 400°C and do not contain lithium, whereas the alkali fluorides do not.

Further experimental work is recommended with the following salts:

1. NaF-ZrF₄ and related ternary mixtures :
 - i. NaF-ZrF₄ (59.5-40.5) *potentially least expensive*
 - ii. ⁷LiF-NaF-ZrF₄ (42-29-29) *very low vapor pressure*
 - iii. RbF-NaF-ZrF₄ (34.5-24-41.5) *lowest melting point*
2. Alkali fluoride salts (e.g., FLiNaK) as a reference salt. These salts will establish the bounding corrosion response, and permit corrosion studies under a wide range of redox conditions.

The corrosion and properties database for BeF₂ salts is rather extensive. BeF₂ salts are expensive, and they impose significant costs in conducting tests. It is likely that much of the information needed for work at temperatures above 750°C can be gathered initially with other inexpensive and less hazardous salts. This leaves the option open for a future selection of BeF₂ salts, should that option prove to be the best one.

7.4 FUTURE WORK

The database for salt thermal conductivity and heat capacity needs significant improvement. In particular, the properties database for ZrF₄-salts is in question and merits further investigation.

An integrated materials design and testing strategy will be required to make the optimal choice of salt based on corrosion metrics. It is recommended that the salt-chemistry, corrosion-chemistry, and alloy-selection studies be conducted as a joint effort.

Although there remain a number of technical issues with respect to molten salt coolants, a better understanding of economic factors for the production of industrial-scale quantities of these materials is even more urgent. It is recommended that a study be done to place the cost of salts for an industrial deployment on a sound footing. At present, only NaF can truly be considered a commodity chemical for the production of salt.

8. REFERENCES

1. D. T. Ingersoll et al., *Status of Preconceptual Design of the Advanced High-Temperature Reactor*, ORNL/TM-2004/104 Oak Ridge National Laboratory, Oak Ridge, TN (2004).
2. C. W. Forsberg et al., "The Advanced High-Temperature Reactor", *Nuclear Engineering International*, p.32, (April 2003).
3. W. R. Grimes, "Molten Salt Reactor Chemistry," *Nuclear Applications and Technology* **8(2)**, pp. 137–155 (1970).
4. W. R. Grimes, *Chemical Research and Development for the Molten-Salt Breeder Reactor*, ORNL/TM-1853, Oak Ridge National Laboratory, Oak Ridge, TN (1967).
5. J. P. Sanders, *A Review of Possible Choices for Secondary Coolants for Molten Salt Reactors*, ORNL CF-71-8-10, Oak Ridge National Laboratory, Oak Ridge, TN (1971).
6. H. F. McMurdie et al., *Phase Diagrams for Ceramists*, National Bureau of Standards multivolume compilation starting in 1964 and continuing to the present, published by the American Ceramic Society.
7. R. E. Thoma, "Phase Diagrams of Binary and Ternary Fluoride Systems," in *Advances in Molten Salt Chemistry*, ed. J. Braunstein et al., Plenum Press, NY, Vol. 3, Chap. 6 (1975).
8. W. R. Grimes et al., "Chemical Aspects of Molten Fluoride Salt Reactor Fuels," in *Fluid-Fueled Reactors*, ed. J. A. Lane et al., Addison-Wesley, NY, Chap. 12 (1958).
9. R. E. Thoma, *Phase Diagrams of Nuclear Reactor Materials*, ORNL-2548, Oak Ridge National Laboratory, Oak Ridge, TN (1959).
10. G. J. Janz, *Molten Salts Handbook*, Academic Press, NY (1967).
11. U.S. Atomic Energy Commission, *Reactor Handbook*, Vol. 4: *Engineering*, ed. S. Mclain and J. H. Martens, Interscience Publishers, NY, p. 841 (1964).
12. K. A. Sense et al., series of articles in *Journal of Physical Chemistry* **61**, p. 337; **62**, pp. 96, 453, 1411 (1957, 1958).
13. D. F. Williams et al., "The Influence of Lewis Acid/Base Chemistry on the Removal of Gallium by Volatility from Weapons Grade Plutonium Dissolved in Molten Chlorides," *Nuclear Technology* **136**, p. 367 (2001).
14. W. R. Grimes, *Reactor Chemistry Division Annual Progress Report for Period Ending December 31, 1965*, ORNL-3913, Oak Ridge National Laboratory, Oak Ridge, TN, p. 27 (1966).
15. D. J. Rogers, T. Yoko, and G. J. Janz, "Fusion Properties and Heat Capacities of the Eutectic LiF-NaF-KF," *J. Chem. Eng. Data* **27**, p. 366 (1982).
16. M. W. Rosenthal et al., *Molten Salt Reactor Program Semi-Annual Progress Report for Period Ending August 31, 1968*, ORNL-4344, Oak Ridge National Laboratory, Oak Ridge, TN, p. 103 (1969)
17. S. Cantor, W. T. Ward, and C. T. Moynihan, "Viscosity and Density in Molten LiF-BeF₂ Solutions," *Journal of Chemical Physics* **50(7)**, p. 2874 (1969).
18. S. I. Cohen, W. D. Powers, and N. D. Greene, *Viscosity Measurements on Molten Fluoride Mixtures*, ORNL-2278, Oak Ridge National Laboratory, Oak Ridge, TN, (1957).
19. C. T. Moynihan and S. Cantor, "Viscosity and Its Temperature Dependence in Molten BeF₂," *Journal of Chemical Physics*, **48(1)**, p.115 (1968).
20. T. Grande, S. Aasland, and S. Julsrud, "Some Comments on the Thermodynamic Aspects of Glass Formation in Fluoride Systems," *Journal of Non-Crystalline Solids* **184**, p.114 (1995).

21. J. Lucas, "Fluoride Glasses," *J. Material Sci.* **24**, p.1 (1989).
22. T. Grande, H. A. Oye, and S. Julsrud, "Viscosity and Density of Molten Barium Zirconate and Related Melts," *J. Non-Crystalline Solids* **161**, p.152 (1993).
23. K. Torlep and H. A. Oye, "Viscosity of Eutectic LiF-NaF-KF," *J. Chem. Eng. Data* **25**, p.16 (1980).
24. E. Veliyulin, A. Voronel, and H.A. Oye, "Universal Features in the Viscosity Behavior of Salt Melts and their Mixtures," *J.Phys. Condens. Matter* **7**, p.4821 (1995).
25. K. Cornwell, "The Thermal Conductivity of Molten Salts," *Journal of Physics D: Applied Physics* **4**, pp. 441–45 (1971).
26. E. McLaughlin, "Thermal Conductivity of Liquids and Dense Gases," *Chemical Reviews* **64**, pp. 389–428 (1964).
27. D. T. Jamieson et al., *Liquid Thermal Conductivity: A Data Survey to 1973*, National Engineering Laboratory, Her Majesty's Stationery Office, Edinburgh (1975).
28. C. H. Gabbard, *Reactor Power Measurement and Heat Transfer Performance in the Molten Salt Reactor Experiment*, ORNL-TM-3002, Oak Ridge National Laboratory, Oak Ridge, TN, p. 23 (1970).
29. J. W. Cooke, *Development of the Variable-Gap Technique for Measuring the Thermal Conductivity of Fluoride Salt Mixtures*, ORNL-4831, Oak Ridge National Laboratory, Oak Ridge, TN (1973).
30. J. W. Cooke, *Experimental Determinations of the Thermal Conductivity of Molten Fluoride Mixtures*, ORNL CF 66-5-1, Oak Ridge National Laboratory, Oak Ridge, TN (1966).
31. U.S. Atomic Energy Commission, *Reactor Handbook*, vol. 4: *Engineering*, ed. S. Mclain and J. H. Martens, Interscience Publishers, NY, p. 53 (1964).
32. M. W. Rosenthal et al., *Development Status of Molten Salt Breeder Reactors*, ORNL-4812, Oak Ridge National Laboratory, Oak Ridge, TN, p. 250 (1972).
33. J. W. Cooke and B. W. Cox, *Forced-Convection Heat Transfer Measurements with a Molten Fluoride Salt Mixture Flowing in a Smooth Tube*, ORNL-TM-4079, Oak Ridge National Laboratory, Oak Ridge, TN (1973).
34. W. R. Gambill, "Fused Salt Thermal Conductivity," *Chemical Engineering* , pp. 129–30, (August 1959).
35. V. Ignatiev et al., "Transport Properties of Molten Salt Reactor Fuel Mixtures," paper presented at Actinide and Fission Product Partitioning Transmutation — 7th Information Exchange Meeting, Jeju, Korea, (October 14–16, 2002).
36. J. McDonald and H. T. Davis, "Determination of the Thermal Conductivities of Several Molten Alkali Halides by Means of a Sheated Hot Wire Technique," *Physics and Chemistry of Liquids* **2**, pp. 119–134 (1971).
37. M. V. Smirnov et al., "Thermal Conductivity of Molten Alkali Halides and Their Mixtures," *Electrochimica Acta* **31**(7), p. 1019 (1987).
38. V. A. Khoklov, "Thermal Conductivity in Cryolitic Melts: New Data and Its Influence on Heat Transfer in Aluminum Cells," *Light Metals* (1998).
39. C. F. Bonilla, "Comparison of Coolants," in *Nuclear Engineering Handbook*, H. Etherington editor, Sect. 9-3, Chap. 6.5, pp. 9–90 (1958).
40. D. T. Ingersoll, *Status of the Physics and Safety Analyses for the Liquid-Salt-cooled Very High-Temperature Reactor (AHTR)*, ORNL/TM-2005/218, Oak Ridge National Laboratory, Oak Ridge, TN (2005).

41. D. E. Robertson et al., *Low-Level Radioactive Waste Classification, Characterization, and Assessment: Waste Streams and Neutron-Activated Metals*, NUREG/CR-6567, PNNL-11659 (2000).
42. United States Geological Service Minerals Yearbooks: <http://minerals.usgs.gov/minerals/pubs/mcs/>
43. W. D. Powers, S. I. Cohen, and N. D. Greene, "Properties of Molten Reactor Fuels and Coolants," *Nuclear Science and Engineering* 17, p. 200 (1963).
44. *Nuclear Science and Engineering* 2, p.797-853: special issue devoted to the ARE (1957).
45. W. R. Grimes and D. R. Cuneo, "Molten Salts as Reactor Fuels," Chapter 17 in *Reactor Handbook, 2nd ed., Vol. 1: Materials*, ed. C. R. Tipton, Jr., Interscience Publishers, Inc., NY (1960).
46. W. B. Cottrell et al., *Operation of the Aircraft Reactor Experiment*, ORNL-1845, Oak Ridge National Laboratory, Oak Ridge, TN (1955).
47. W. D. Manly et al., *ARE–Metallurgical Aspects*, ORNL-2349, Oak Ridge National Laboratory, Oak Ridge, TN (1957).
48. W. B. Cottrell, *Disassembly and Postoperative Examination of the Aircraft Reactor Experiment*, Oak Ridge National Laboratory Report, ORNL-1868, Oak Ridge National Laboratory, Oak Ridge, TN (1958).
49. R. B. Evans III, J. H. DeVan, and G. M. Watson, *Self-Diffusion of Chromium in Nickel-Base Alloys*, ORNL-2982, Oak Ridge National Laboratory, Oak Ridge, TN (1960).
50. J. H. DeVan and R. B. Evans III, *Corrosion Behavior of Reactor Materials in Fluoride Salt Mixtures*, ORNL/TM-328, Oak Ridge National Laboratory, Oak Ridge, TN (1962).
51. G. M. Adamson, R. S. Crouse, and W. D. Manly, *Interim Report on Corrosion by Zirconium-Base Fluorides*, ORNL-2338, Oak Ridge National Laboratory, Oak Ridge, TN (1961).
52. J. H. DeVan, "Effect of Alloying Additions on Corrosion Behavior of Nickel-Molybdenum Alloys in Fused Fluoride Mixtures," University of Tennessee Thesis, August 1960, see also Oak Ridge National Laboratory Report ORNL/TM-2021, Oak Ridge National Laboratory, Oak Ridge, TN (1969).
53. J. H. DeVan and R. B. Evans III, "Corrosion Behavior of Reactor Materials in Fluoride Salt Mixtures," pp. 557–579 in *Corrosion of Reactor Materials Vol. II, Proceedings of the Conference on Corrosion of Reactor Materials*, June 4–8, 1962, IAEA, Vienna (1961).
54. W. H. Jordan et al., *Aircraft Nuclear Propulsion Project Quarterly Progress Report*, ORNL-2387, Oak Ridge National Laboratory, Oak Ridge, TN (1958).
55. W. R. Grimes, pp. 96–99 in W.H. Jordan et al., *Aircraft Nuclear Propulsion Project Quarterly Progress Report for Period Ending June 10, 1956*, ORNL-2106, Oak Ridge National Laboratory, Oak Ridge, TN (1956).
56. H. E. McCoy and B. McNabb, *Postirradiation Examination of Materials from the MSRE*, Oak Ridge National Laboratory Report, ORNL/TM-4174, Oak Ridge National Laboratory, Oak Ridge, TN (1972).
57. M. W. Rosenthal, *The Development Status of Molten-Salt Breeder Reactors*, ORNL-4812, Oak Ridge National Laboratory, Oak Ridge, TN (1972).
58. W. D. Manly et al., "Metallurgical Problems in Molten Fluoride Systems," *Progress in Nuclear Energy*, Series IV 2, pp. 164–179 (1960).
59. H. E. McCoy, Jr., *Status of Materials Development for Molten Salt Reactors*, ORNL-TM-5920, Oak Ridge National Laboratory, Oak Ridge, TN (1978).

60. J. R. Keiser, *Compatibility Studies of Potential Molten-Salt Breeder Reactor Materials in Molten Fluoride Salts*, ORNL-TM-5783, Oak Ridge National Laboratory, Oak Ridge, TN (1977).
61. J. R. Keiser, *Status of Tellurium-Hastelloy N Studies in Molten Fluoride Salts*, ORNL-TM-6002, Oak Ridge National Laboratory, Oak Ridge, TN (1977).
62. J. H. Shaffer, *Preparation and Handling of Salt Mixtures for the Molten Salt Reactor Experiment*, ORNL-4616, Oak Ridge National Laboratory, Oak Ridge, TN (1971).
63. R. B. Briggs, *Molten Salt Reactor Program Semiannual Progress Report for Period Ending Feb 28, 1962*, ORNL-3282, Oak Ridge National Laboratory, Oak Ridge, TN (1962).
64. W. R. Grimes, "Materials Problems in Molten Salt Reactors," Chapter 7 in *Materials and Fuels for High-Temperature Nuclear Energy Applications*, Proceedings of the National Topical Meeting on the American Nuclear Society, San Diego, April 11–13, 1962, ed. M. T. Simnad and L. R. Zumwalt, M.I.T. Press, Cambridge, Mass.
65. C. F. Baes, "The Chemistry and Thermodynamics of Molten Salt Reactor Fuels", *J. Nuclear Materials*, **51(1)**, p. 149, (1974).
66. L. S. Richardson, D. E. Vreeland, and W. D. Manly, *Corrosion by Molten Fluorides*, ORNL-1491, Oak Ridge National Laboratory, Oak Ridge, TN (1953).
67. W. H. Jordan et al., *Aircraft Nuclear Propulsion Project Quarterly Progress Report for period ending March 10, 1954*, ORNL-1692, p.69, Oak Ridge National Laboratory, Oak Ridge, TN (1954).
68. "Chemical Reactions in Molten Salts: Stability of Structural Metal Fluorides," section in series of *Aircraft Nuclear Propulsion Project Quarterly Progress Reports*: ORNL-1816, 1864, 1896, 1947, 2012, 2257, 2221, 2274, 2387, Oak Ridge National Laboratory, Oak Ridge, TN (1955–1958)
69. W. H. Jordan et al., *Aircraft Nuclear Propulsion Project Quarterly Progress Report for period ending June 10, 1956*, ORNL-2106, Oak Ridge National Laboratory, Oak Ridge, TN, p.95, (1956).
70. W. H. Jordan et al., *Aircraft Nuclear Propulsion Project Quarterly Progress Report for period ending Sept. 10, 1956*, ORNL-2157, Oak Ridge National Laboratory, Oak Ridge, TN, p.107, (1956).
71. W. H. Jordan et al., *Aircraft Nuclear Propulsion Project Quarterly Progress Report for period ending December 31, 1956*, ORNL-2221, Oak Ridge National Laboratory, Oak Ridge, TN, p.125 (1957).
72. W. H. Jordan et al., *Aircraft Nuclear Propulsion Project Quarterly Progress Report for period ending September 10, 1956*, ORNL-2157, Oak Ridge National Laboratory, Oak Ridge, TN, p.145, (1956).
73. W. H. Jordan et al., *Aircraft Nuclear Propulsion Project Quarterly Progress Report for period ending December, 31, 1956*, ORNL-2221, Oak Ridge National Laboratory, Oak Ridge, TN, p.182, (1957).
74. J. R. Keiser et al., *The Corrosion of Type 316 Stainless Steel to Li_2BeF_4* , ORNL/TM-5782, Oak Ridge National Laboratory, Oak Ridge, TN (1977).
75. G. D. Del Cul et al., "Redox Potential of Novel Electrochemical Buffers useful for Corrosion Prevention in Molten Fluorides," *Proceedings of the Thirteenth International Symposium on Molten Salts Held during the 201st meeting of the Electrochemical Society*. Philadelphia, PA, May 12–17, 2002.

76. W. D. Manley et al., "Construction Materials for Molten-Salt Reactors," in *Fluid-Fueled Reactors*, ed. J. A. Lane et al., Addison-Wesley, NY, Chap. 13 (1958)
77. D. F. Williams, et al., "Research on Molten Fluorides as High Temperature Heat Transfer Agents," *Proceedings of GLOBAL 2003*, New Orleans, USA, Nov.16–20, 2003.

APPENDIX

Table A.1. Summary of corrosion testing results for salts without uranium

Loop #	Alloy	Salt	Duration [h]	T_{max} [°C]	Corrosion depth [mil]	ORNL report # or [reference]
116	316SS	FLiNaK	500	815	4	1294
119	316SS	FLiNaK + NaK	500	815	2	1294
347	Inconel	50NaF-50ZrF ₄	3000	815	11	1692
518	Inconel	NaF-ZrF ₄	3000	815	11	2338
346	Inconel	50NaF-50ZrF ₄	2000	815	9	1692
519	Inconel	NaF-ZrF ₄	2000	815	12.5	1692
78	Inconel	FLiNaK	1000	815	13	1294, 2337
	Inconel	NaF-ZrF ₄	1000	815	3	[76]
278	Inconel	NaF-ZrF ₄	1000	815	5	2338
399	Inconel	NaF-ZrF ₄	1000	815	10	2338
	Inconel	60NaF-40ZrF ₄	1000	815	5	CF-57-9-35
	Inconel	50NaF-50Be ₂	1000	815	8	CF-57-9-35
	Inconel	70NaF-30BeF ₂	1000	815	6	CF-57-9-35
	Inconel	24LiF-53NaF-23BeF ₂	1000	815	5	CF-57-9-35
	Inconel	36LiF-49NaF-15BeF ₂	1000	815	3	CF-57-9-35
	Inconel	74LiF-26ThF ₄	1000	815	6	CF-57-9-35
517	Inconel	NaF-ZrF ₄	822	815	5.5	2338
337	Inconel	NaF-ZrF ₄	575	815	8	2338
214	Inconel	FLiNaK + NaK	500	815	3	1294
230	Inconel	36NaF-18KF-46ZrF ₄	500	815	10	1375
348	Inconel	50NaF-50ZrF ₄	500	815	5.5	1692
	Inconel	FLiNaK	500	815	7	1816
934	Inconel	60NaF-40ZrF ₄	500	815	5	2157
935	Inconel	60NaF-40ZrF ₄	500	815	5	2157
	Inconel	NaF-BeF ₂	500	815	10	[76]
	Inconel	LiF-NaF-BeF ₂	500	815	5	[76]
246	Inconel	52NaF-48ZrF ₄	500	815	8	2337
262	Inconel	57NaF-43BeF ₂	500	815	9	2337
277	Inconel	50NaF-50ZrF ₄	500	815	5	2337

Loop #	Alloy	Salt	Duration [h]	T_{max} [°C]	Corrosion depth [mil]	ORNL report # or [reference]
276	Inconel	NaF-ZrF ₄	500	815	8	2338
277	Inconel	NaF-ZrF ₄	500	815	4	2338
336	Inconel	NaF-ZrF ₄	500	815	6	2338
341	Inconel	NaF-ZrF ₄	500	815	5.5	2338
342	Inconel	NaF-ZrF ₄	500	815	6	2338
516	Inconel	NaF-ZrF ₄	500	815	6	2338
338	Inconel	NaF-ZrF ₄	500	815	6	2338
411	Inconel	NaF-ZrF ₄	250	815	4.5	2338
410	Inconel	NaF-ZrF ₄	100	815	4	2338
400	Inconel	NaF-ZrF ₄	50	815	3	2338
1181	Inconel	71LiF-29ThF ₄	8760	732	6.5	2684
1239	Inconel	71LiF-16BeF ₂ -13ThF ₄	8760	732	7.5	2973
9377-6	Inconel	71LiF-16BeF ₂ -13ThF ₄	13155	704	13	3215
1188	Inconel	35LiF-27NaF-38BeF ₂	8760	677	9	2723
1210	Inconel	71LiF-29ThF ₄	8760	677	5	2799
1235	Inconel	71LiF-16BeF ₂ -13ThF ₄	7789	677	4	2973
1214	Inconel	FLiNaK	4673	677	13	2684
1169	Inconel	71LiF-29ThF ₄	1000	677	1	2474
1177	Inconel	71LiF-29ThF ₄	1000	677	1.5	2474
1173	Inconel	58NaF-35BeF ₂ -7ThF ₄	1000	677	4	2474
1176	Inconel	58LiF-35BeF ₂ -7ThF ₄	1000	677	1	2474
1234	Inconel	71LiF-16BeF ₂ -13ThF ₄	1000	677	1	2799
9344-2	Inconel	FLiNaK	8760	649	8	2890
9344-2	Inconel	FLiNaK	8735	649	8	3215
1172	Inconel	35LiF-27NaF-38BeF ₂	1000	607	2	2474
1175	Inconel	FLiNaK	1000	607	1	2474
LDRD	INOR-8	FLiNaK	3048	815	0.1	[77]
1209	INOR-8	71LiF-29ThF ₄	8760	732	0	2799
1216	INOR-8	58LiF-35BeF ₂ -7ThF ₄	8760	732	1	2973
1240	INOR-8	71LiF-16BeF ₂ -13ThF ₄	8760	732	0	2973
MSRP7	INOR-8	71LiF-16BeF ₂ -13ThF ₄	20000	704	1	3215
MSRP8	INOR-8	58LiF-35BeF ₂ -7ThF ₄	9633	704	0	3215

Loop #	Alloy	Salt	Duration [h]	T_{max} [°C]	Corrosion depth [mil]	ORNL report # or [reference]
15A	INOR-8	73LiF-2BeF ₂ -25ThF ₄	39476	677	0.05	<i>TM-4286</i>
1208	INOR-8	FLiNaK	8760	677	1	<i>2799</i>
1190	INOR-8	58NaF-35BeF ₂ -7ThF ₄	8760	677	1	<i>2799</i>
1233	INOR-8	71LiF-16BeF ₂ -13ThF ₄	8760	677	0	<i>2973</i>
1213	INOR-8	71LiF-29ThF ₄	3114	677	0	<i>2626</i>
15	INOR-8	73LiF-2BeF ₂ -25ThF ₄	2003	677	0	<i>TM-4286</i>
1165	INOR-8	FLiNaK	1340	677	0	<i>2551</i>
1164	INOR-8	58NaF-35BeF ₂ -7ThF ₄	1000	677	0	<i>2551</i>
1221	INOR-8	71LiF-29ThF ₄	1000	677	0	<i>2626</i>
1228	INOR-8	71LiF-16BeF ₂ -13ThF ₄	1000	677	0	<i>2723</i>
MSRE	INOR-8	67LiF-33BeF ₂	26000	649	0	<i>TM-4174</i>
9354-3	INOR-8	35LiF-27NaF-38BeF ₂	19942	649	0	<i>3215</i>
1194	INOR-8	FLiNaK	1000	607	0	<i>2551</i>
1195	INOR-8	35LiF-27NaF-28BeF ₂	1000	607	0	<i>2551</i>

